DISTRIBUTION IN ENERGY AND ANGLE OF FAST NEUTRONS SCATTERED FROM IRON

APPROVED:

[redacted]

APPROVED:

[redacted]

Dean of the Graduate School

DISTRIBUTION IN ENERGY AND ANGLE OF FAST NEUTRONS SCATTERED FROM IRON

DISSERTATION

Presented to the Faculty of the Graduate School of

The University of Texas in Partial Fulfillment

of the Requirements

For the Degree of

DOCTOR OF PHILOSOPHY

By

Charles Patrick Cadenhead, B. S., M. A.

Austin, Texas

June 1953

PREFACE

The advice and encouragement of Dr. R. N. Little, Jr. is gratefully acknowledged. Appreciation is also expressed to all members of the Cockroft Walton group. In particular, the help of J. E. Wills and H. R. Dvorak was invaluable.

C. P. C.

The University of Texas
Austin, Texas
June, 1953

TABLE OF CONTENTS

CHAPTER I

INTRODUCTION

In the field of neutron physics progress has been slow because of the lack of a really good neutron detector. Many types of detectors have been used with various results. The ideal detector would combine high efficiency with either good energy resolution or detection of all energies with equal efficiency. So far this ideal detector has not been realized. The two primary principles which have been used in detection are the observation of the recoil of nuclei (principally hydrogen and helium) from a collision with a neutron and the activation of nuclei by neutron capture with later emission of particles which can be detected. The observation of proton recoils either in a photographic emulsion or in a cloud chamber gives the best results on measurements of energy of the neutrons. Both of these methods suffer from the long times involved in obtaining the desired information, not only from the exposure-to-radiation time, but also because of the generally much longer time required to extract the results from the films used. Ionization chambers and other types of recoil counters have also been used, but they too suffer from very low efficiencies

or low resolutions. Activation cross sections for fast neutrons are, in general, quite low, and their energy dependence is seldom well known.

In the last few years the advent of scintillation counters has given considerable emphasis to this field of physics, since it is quite feasible to get efficiencies of the order of 10 to 50% for the detection of neutrons. Efficiencies of this order of magnitude have made feasible the performance of experiments which would have taken a prohibitive amount of time otherwise.

The present experiment is an attempt to analyze the energy distribution of the neutrons scattered at a particular angle when a beam of monoenergetic neutrons is incident on the scatterer and hence to measure: (1) differential angular elastic scattering cross sections, (2) differential angular inelastic scattering cross sections and (3) analyze the energy distribution of the scattered neutrons.

CHAPTER II

SCATTERING PROCESSES

There are two processes through which neutrons may lose energy in passing through matter. The first of these is the so-called elastic scattering and the second is inelastic scattering. These two subdivisions are made on the basis of the energy losses involved. If the energy loss in a collision is exactly that which can be accounted for by assuming the conservation of momentum of the two particles, then the scattering is called elastic. If the energy loss is more than can be accounted for in this way, the scattering is called inelastic.

Elastic scattering can be subdivided into two groups, potential elastic scattering and resonant or capture elastic scattering. The behavior of the potential elastic scattering can be calculated using the techniques of optical diffraction theory.[1] The angular

---

1. Feld, Feshbach, Goldberger, Goldstein, Weisskopf, "Final Report of the Fast Neutron Data Project", NYO-636, U. S. Atomic Energy Commission.

---

distribution of the scattered neutrons with this treatment shows a strong maximum in the forward direction and decreases to a more or less constant value in the

back direction where the major effect is that of reflection scattering. Capture elastic scattering, on the other hand is actually a special case of inelastic scattering, in that the neutron actually "enters" the nucleus but is re-emitted from the nucleus with the same energy it originally possessed, except for the energy of the recoil nucleus. This type of scattering may be isotropic under certain conditions which will be discussed under inelastic scattering.

Inelastic scattering occurs when a neutron enters the nucleus and is re-emitted with a loss of energy leaving the residual nucleus in a state of excitation. The residual nucleus generally decays to the ground, or original level, by subsequent emission of one or more gamma rays. Inelastic scattering is the main source of energy loss for high energy neutrons and heavy nuclei, while elastic scattering is more effective for low energy neutrons and light nuclei.

One of the better summaries to date of the theoretical work on scattering cross sections to date has been made by Feld, et al.[2] Their work has served as a

---

2. Feld, Feshbach, Goldberger, Goldstein, Weisskopf, ibid.

---

guide for some of the following remarks.

For calculation and discussion purposes, it is convenient to divide inelastic scattering processes into three classes, distinguished by the possibility of applying statistical theory to the problem, that is, whether there are a large number of excitation levels available or not. The characteristics of the three classes are:

I. A statistical approach is not valid for the compound or the residual nucleus.

II. A statistical approach is valid for the compound nucleus but is not valid for the residual nucleus.

III. A statistical approach is valid for both the compound and the residual nucleus.

In terms of the masses of the nuclei in the energy range used, nuclei with masses less than approximately 20 belong to class I, nuclei with masses between 20 and 100 as well as the heavy "magic" nuclei belong to class II, and the heavy nuclei belong to class III. Iron has a mass of 56 and the 2.8 mev. of the incident neutron energy plus the binding energy of the neutron give a high enough excitation level so that many levels should be excited in the compound nucleus, while only discrete levels have been observed in the residual

nucleus.[3,4] Nuclei of class II should yield valuable

3. Day, R. B., Phy. Rev. 89, 908 (1953).
4. Elliot, L. G. and Deutsch, M., Phy. Rev. 63, 321 (1943).

information on nuclear structure since they have widely spaced levels in the residual nucleus. The inelastically scattered neutrons will emerge in groups with energy losses corresponding to the energies of the various excited levels and with numbers proportional to the total cross section for the excitation of each level.

It is also of great interest to observe the angular distribution of the neutrons from each of the excited levels. According to Feld, et al.[5], the angular

5. Feld, Feshbach, Goldberger, Goldstein, Weisskopf, op cit.

distribution (for class II nuclei) should be an even function of cos θ where θ is the angle of emission referred to the direction of the incident neutron. This is a consequence of the assumption that the statistical model of the nucleus is valid for the compound nucleus and failure of this symmetry would indicate that the statistical model is not valid for the compound nucleus. One further result can be obtained from

the angular distribution. The highest power of cos Θ that can appear in the angular distribution is determined by the angular momentum quantum number of either the incident or the emitted neutron with respect to the nucleus. The information on angular distribution of scattered neutrons, coupled with information obtained in other ways, should lead to unambiguous assignments of spin and parity to the levels of nuclei.

CHAPTER III

APPARATUS

There are two nuclear reactions which will yield large numbers of neutrons at low bombarding energy. The D(d,n) reaction, symbolically

$$_1D^2 + {}_1D^2 \rightarrow {}_2He^3 + {}_0n^1 + 3.268 \text{ mev.}$$

yields neutrons of energy approximately 2.5 mev. The T(d,n) reaction, symbolically

$$_1D^2 + {}_1T^3 \rightarrow {}_2He^4 + {}_0n^1 + 17.58 \text{ mev.}$$

yields neutrons of approximately 14 mev. The first of these reactions was used in the present experiment.

The 100 kv. linear accelerator in the University of Texas Physics Department was used to accelerate deuterium ions to energies of 100,000 volts. These deuterium ions were then allowed to strike the bottom of a thin copper sphere where some of the ions were occluded into the copper and other of the ions reacted with the occluded ions, whereupon the D(d,n) reaction took place yielding neutrons of approximately 2.8 mev. in the forward direction. This type of target was used instead of a specially prepared target because of the ease of preparation. The total number of neutrons produced was of the order of 10^6 per second at an unanalyzed beam current of 500 microamperes.

The emitted neutrons were not completely monoenergetic because of three factors: first, a "thick" target is the source of the neutrons. Since the energy of the neutrons is a function of the bonbarding energy, there will be some neutrons of slightly lower energy. Second, an unanalyzed beam of deuterons was used, which means that there were deuterons participating in the reaction which had not only 100 kev. from atomic ions but also some of the 50 kev. energy from molecular ions, some of 33 kev. energy, etc. These two effects on the neutron energy are comparatively small (the difference between half-maximum points of the neutron energy peak having been measured to be 0.3 mev.[6]) because of the

---

6. Brundage, R. S., "Total Cross Section of Aluminum for D(d,n) Neutrons", unpublished M. A. Thesis, University of Texas, June 1952.

---

rapidly increasing yield of the reaction as the energy of the ions is increased. The third factor in the spread of the energy of the neutrons is the variation of the energy of neutrons as a function of the angle of neutron emission with respect to the incident deuteron beam. This latter effect was minimized by taking advantage of the symmetry of the energy variation about the axis of the deuteron beam by using circular ring scatterers. It was also desirable to allow some small

variations of neutron energy in order to take advantage of the much larger fluxes of neutrons available when an unanalyzed beam and thick targets were used.

From the early days of nuclear physics it was realized that nuclear particles would produce small amounts of light when they struck certain fluorescent substances. While this phenomenon was used to a large extent in early experiments, it bacame of small practical use for many years following the development of counter tubes. In recent years the development of the electron multiplier type of tube, which can give tremendous amplification of the current pulses produced by photoelectrons ejected from the cathode of the tube by light quanta, has changed the scintillation method from a state of mere interest to one of great usefulness in every nuclear physics laboratory. The electron photomultiplier has been the means of counting neutrons at rates and efficiencies heretofore unheard of. The first scintillation counters consisted of screens covered with a thin layer of zinc sulfide with the scintillation light pulses from alpha rays being observed visually. This is indeed a far cry from the present scintillation counter systems which can differentiate between pulses coming 10^{-8} sec. apart and can measure the total amount of light from each pulse quite

accurately.

In the last few years several experimenters[7,8,9]

7. Hofstadter, R., Nucleonics 6, No. 5, 70 (1950).

8. Kallmann, H. and Furst, M., Phy. Rev. 79, 857 (1950).

9. Jordan, W. H. and Bell, P. R., Nucleonics 5, No. 4, 30 (1949).

have measured the efficiencies of various substances as scintillators. Certain types of scintillators operate best for counting one type of particle while others operate better for counting other types of particles. In particular, for counting neutrons it is desirable, in most cases, to use some hydrogenous material for the bulk, at least, of the scintillator, although it may be necessary to put small amounts of other material in the detector to produce a higher light production per scintillation. The hydrogenous material is desirable because of the fairly high cross section of protons for neutrons, and because the recoil protons can receive the most energy from the neutrons per collision.

Pure liquids make very poor scintillating material. However, if solutions are used, then it is possible to get strong fluorescence which has the spectral characteristics of the solute molecules.[10] For many purposes

10. Falk, C. E. and Poss, H. L., Am. Jour. Phy. 20, 429 (1952).

liquid scintillators are very useful, since one of the big problems of solid scintillators was the production of good crystals which were as large as desired. The use of liquid scintillators allows the counter size to be as large as desired within the limits of self-absorption and other effects. Also the production of various shapes with liquids is considerably easier than with some of the solid crystals which are used.

The scintillator used in this experiment was of the liquid type, consisting of a solution of five grams of terphenyl per liter of m-xylene.[11,12] The terphenyl

---

11. Dvorak, H. R., "Total Cross Sections of Bromine, Chlorine, Sodium and Titanium", Ph. D. Dissertation, May, 1953 (to be published).

12. Schaeffer, N. M., "Scattering of D(d,n) Neutrons from Plane Slabs", Ph. D. Dissertation, May, 1953 (unpublished).

---

furnishes the scintillation material while the xylene furnishes the hydrogenous carrier. After mixing the solution, it was placed in a glass holder which was then sealed with a teflon stopper. The glass and the teflon are desirable because of their inertness with respect to the solution. If materials are used to contain the solution which will react with or dissolve in the solutions, the liquid soon becomes contaminated with a consequent loss of efficiency and will eventually

have to be replaced. The glass cell was a cylinder 5.1 cm. in diameter and 5 cm. long. One end was concave to match the curvature of the 5819 photomultiplier and the other end was correspondingly convex.

After the glass container had been sealed, it was optically coupled to the 5819 photomultiplier tube with a Dow Corning type 200 fluid. The glass cell was then wrapped with crinkled aluminum foil for better light collection at the photocathode, and the cell and tube were wrapped with black photographic tape to prevent extraneous light from reaching the photocathode and causing spurious pulses. A 2 mm. thick lead shield was then placed over the scintillator head to attenuate any x-rays coming from the accelerator. Figure 1 is a block diagram of the circuitry involved.

Since the current multiplication of the photomultiplier tube is extremely high, it is necessary to keep the voltage on the tube as stable as possible. The high voltage supply for the electron multiplier tube followed the design of the Oak Ridge Dwg. Q-1144-1 power supply. The voltage applied to the photomultiplier tube was checked frequently with a Rubicon potentiometer arrangement and was found to be extremely stable after the resistors and the voltage dividers were allowed to reach stable temperature. If the

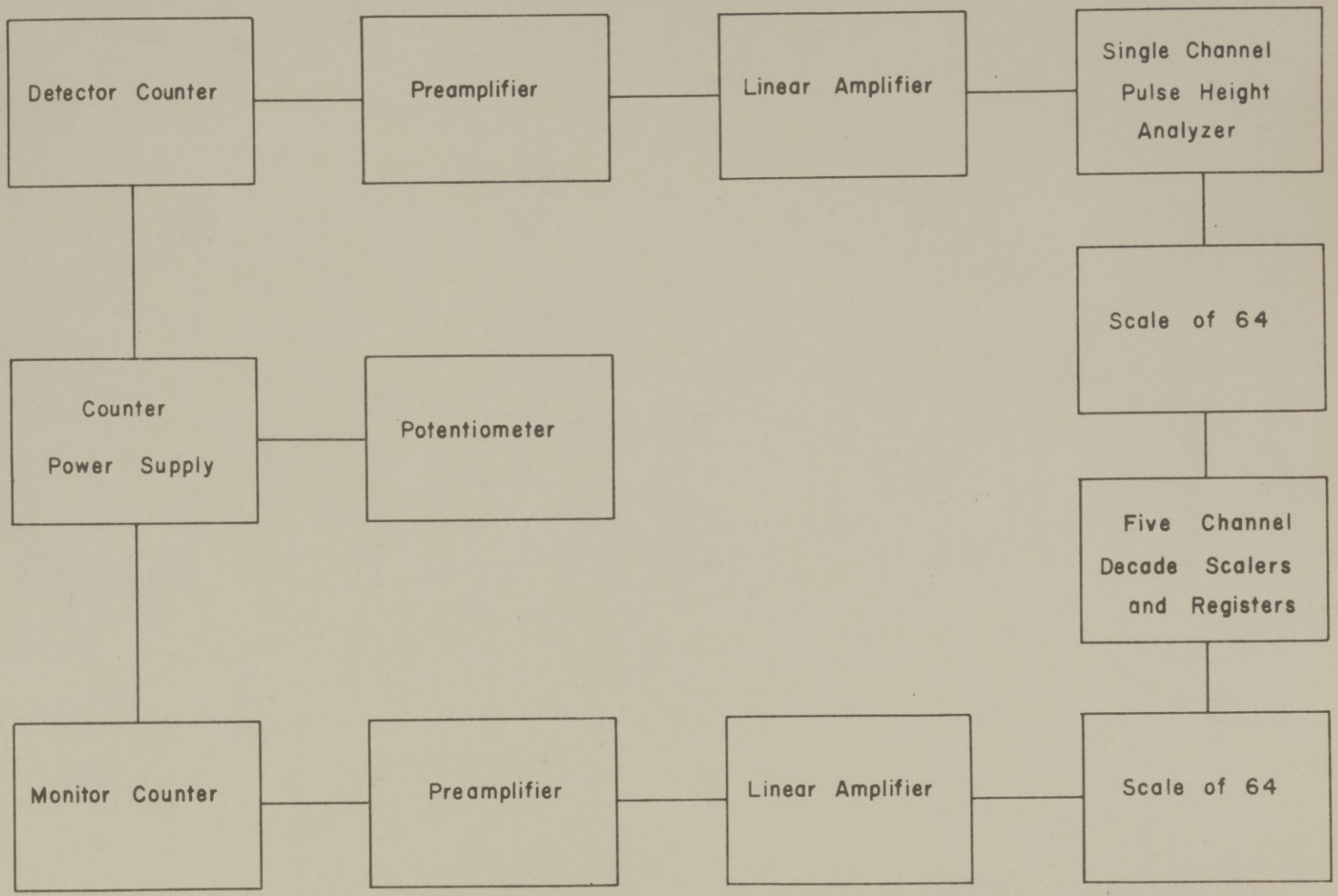

FIGURE I. BLOCK DIAGRAM OF EQUIPMENT

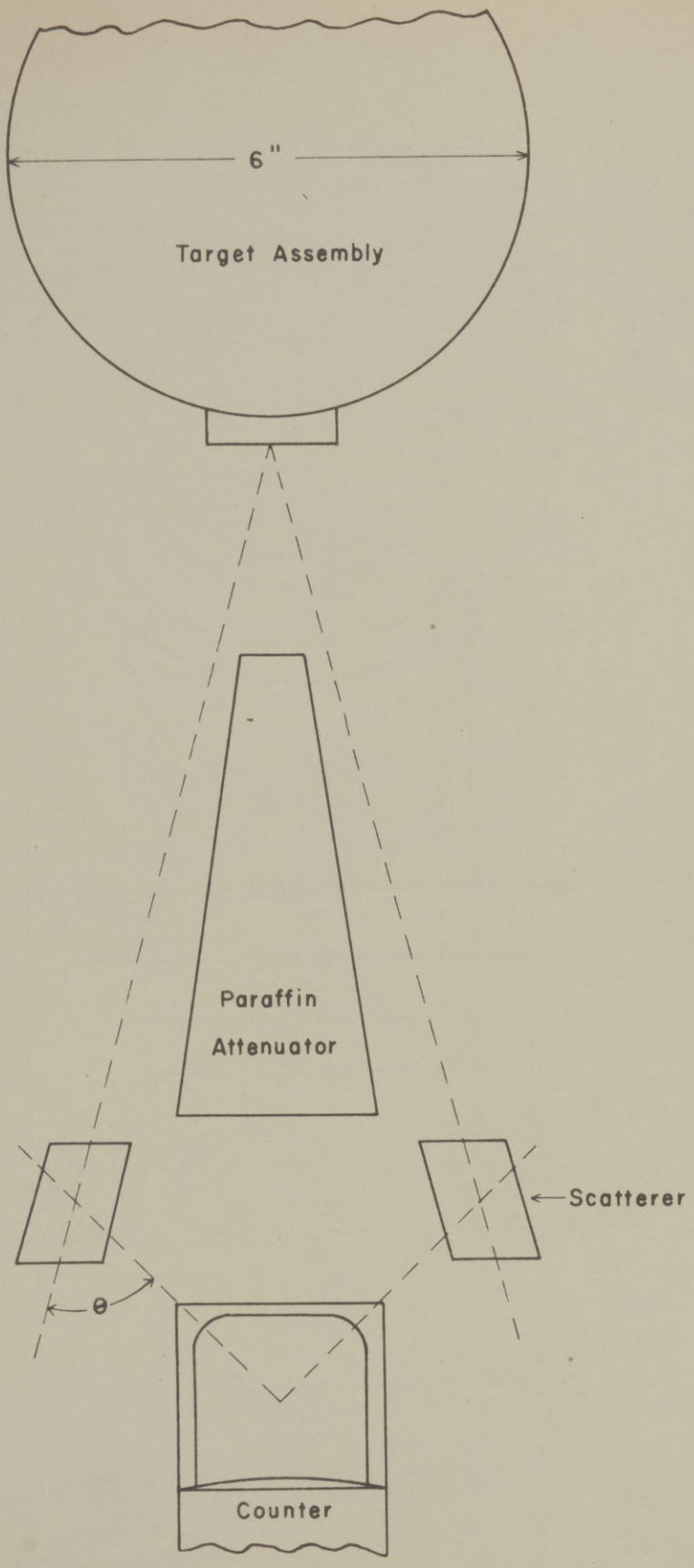

FIGURE 2. GEOMETRY OF EXPERIMENT

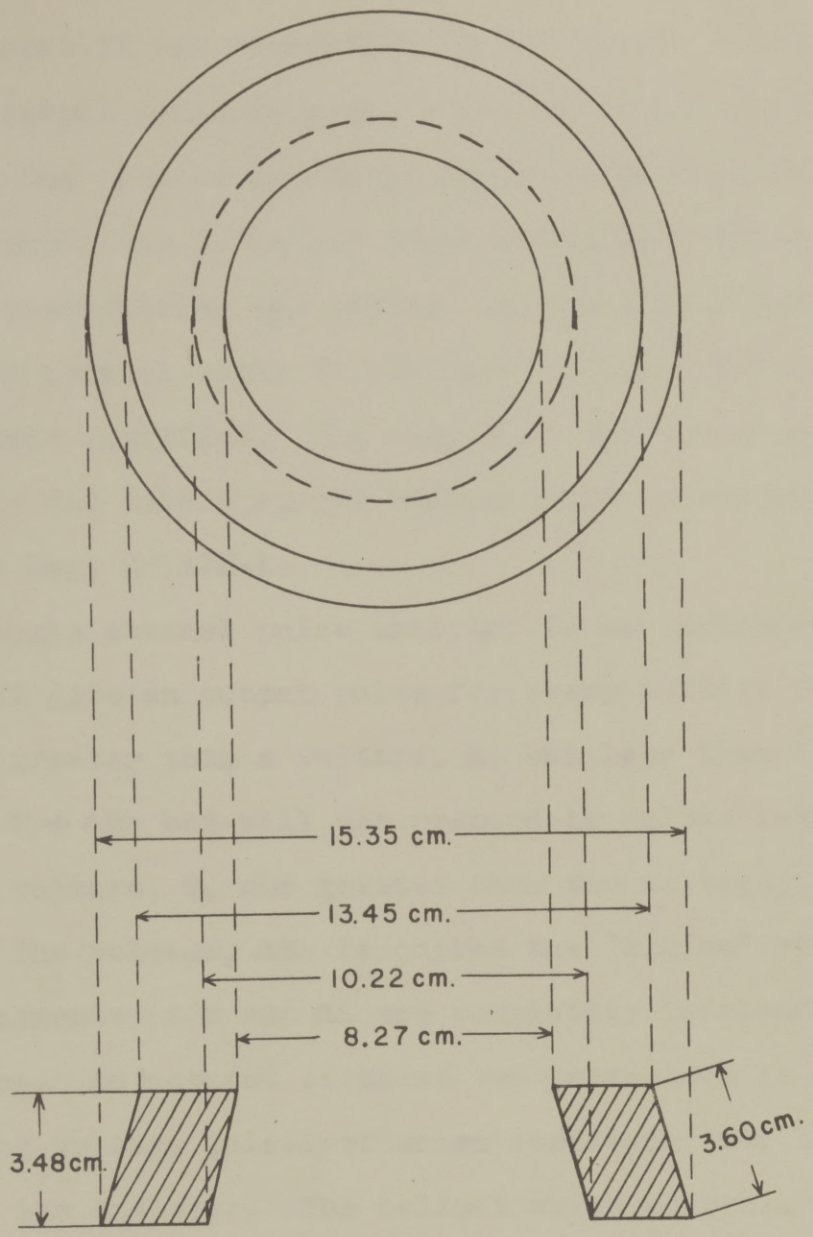

FIGURE 3. IRON SCATTERER

voltage was found to be different by more than a tenth of a per cent it was readjusted to the proper value.

The output pulse from the anode of the photomultiplier was fed into an impedance matching cathode follower preamplifier. The low impedance output pulse from the preamplifier was carried by a six foot length of RG-71/U coaxial cable to the input of the Atomic 204-B linear amplifier. The output of the linear amplifier was fed into a single channel pulse analyzer, Oak Ridge Dwg. Q-1192-1.

A single channel pulse analyzer is an instrument which will give an output pulse for every voltage pulse which is greater than a voltage, E, but less than a voltage, $E + \Delta E$; but will not respond to pulses less than the voltage, E, nor greater than the voltage, $E + \Delta E$. The voltage, ΔE, is called the "window" width. The adjustments of E and ΔE are completely independent operations. Adjustment of these two parameters is made by feeding voltage pulses of known amplitude into the input of the analyzer. The helipot which controls E is calibrated by observing the minimum setting at which pulses will be counted. The helipot which controls ΔE is calibrated by observing the difference between the minimum setting of E at which pulses will be counted and the maximum setting of E at which pulses will be

counted. The actual choice of a ΔE for a particular experiment will be determined by a compromise between the resolution desired and the time required to obtain a reasonable number of counts. If ΔE is made too large, then details of the spectrum may be lost. On the other hand, if ΔE is made too small, the length of time required to obtain small statistical variations is prohibitive.

The output pulses from the single channel analyzer are fed into an Atomic Model 101-M scaler. The output of the scaler is in turn fed into a Berkeley Model 3501 five channel decade counter and register.

The neutron flux was monitored at all times by a similar counter system with the exception that all pulses above a certain height were recorded. The discriminator of the Atomic amplifier was used instead of the single channel analyzer for setting the minimum height pulses counted. The switches of the scalers for the detector and for the monitor were mechanically ganged together so that they could be operated simultaneously. A Standard electric timer was used to measure the time of each run.

CHAPTER IV

PROCEDURE

The first step in the operation of the single-channel differential pulse height analyzer is to calibrate the width of the counting channel as a function of the pulse height control. Pulses of constant height and frequency are fed into the input of the analyzer. The "discriminator output" jack of one of the scalers is a convenient source of such pulses when the scaler is operated on the 60 cycle test position. The analyzer is set on the differential position and the channel width control (ΔE) is set for the maximum width. The discriminator (E) control is turned slowly until pulses are counted. The maximum position of E and the minimum position of E at which pulses are still counted are noted. Since the ΔE dial is fairly linear, the dial can then be roughly set to the desired width. The adjustment of the ΔE control is then completed by carefully noting the points at which the counting rate falls off to one half the maximum value on each side and adjusting the ΔE control until it corresponds to the desired width. The analyzer is now ready to be reconnected to the output of the linear amplifier and put into operation. It is worth noting that the

linear amplifier and the pulse height analyzer should be allowed to warm up for several hours before being put into operation. Since the voltages in the scalers are not as critical, a few minutes of warm-up time suffice for them.

Voltage is applied to the 5819 photomultiplier tube, and the voltage divider supplying the various voltages to this tube is allowed to reach an equilibrium condition, after which the voltage is measured by means of the Rubicon potentiometer. Background counting rates are measured with the high voltage of the accelerator on but with no beam current.

Two different types of runs are made. First, the counter is placed in position and the counting rate as a function of the discriminator setting, E, (called hereafter the "discriminator spectrum") is obtained. All runs are made by first taking the counting rate with the scatterer in, then removing the scatterer and again obtaining the counting rate. The difference between these two intensities (called δI), all other conditions being constant, is due to the presence of the scatterer. After the discriminator spectrum has been obtained, a decision must be made as to where the discriminator should be set in order to obtain the desired angular scattering cross sections. Then the second

type of run is made, in which the discriminator is fixed at one or more values, and the counter position is varied so as to vary the average angle of scattering. All counting rates were divided by the counting rate obtained on a similar scintillation counter (the monitor) which was placed a distance of 55 cm. from the source of neutrons. The counting rates are then given as counts/monitor count which nullifies the effect of variations in the number of neutrons from the target for different "runs". The count switches of the two counters were operated at the same time, thus preventing small errors in time measurement from affecting the final results.

CHAPTER V

ANALYSIS OF DATA

Baldinger, Huber and Staub[13] first pointed out

13. Baldinger, Huber and Staub, Helvetia Physica Acta 11, 245 (1938).

that the distribution in energy of recoil protons from fast neutrons bears a very simple relationship to the distribution in energy of the neutrons, and that this relationship can be used to distinguish between elastically and inelastically scattered neutrons. The scattering of fast neutrons by protons has been shown[14,15,16,17] to be isotropic in the center of mass

14. Kruger, Shoupp and Slattman, Phy. Rev. 52, 678 (1937).

15. Bonner, T. W., Phy. Rev. 52, 685 (1937).

16. Coon, J. H. and Barschall, H. H., Phy. Rev. 70, 592 (1946).

17. Barschall, H. H. and Taschek, R. F., Phy. Rev. 75, 1819 (1949).

system. Under these conditions, the fraction dN of protons scattered into a segment of a spherical surface defined by the angles ϕ and $\phi + d\phi$ (where ϕ is the angle between the incident neutron and the scattered proton) is

$$dN = \frac{2\pi N_0 \sin\phi \, d\phi}{4\pi} = \frac{N_0 \sin\phi \, d\phi}{2}$$

where N_0 is the total number of protons scattered. When transformed to the laboratory system, since $\phi = 2\theta$ where θ is the corresponding angle in the laboratory system, this expression becomes

$$dN = N_0 \sin 2\theta \, d\theta = 2N_0 \sin\theta \cos\theta \, d\theta.$$

Now the energy of the recoil proton in the laboratory system E_p is

$$E_p = E_n \cos^2\theta$$

where E_n is the energy of the incident neutron. Hence

$$dE_p = -2E_n \cos\theta \sin\theta \, d\theta$$

and

$$\frac{dN_p}{dE_p} = \frac{2N_0 \sin\theta \cos\theta \, d\theta}{-2E_n \cos\theta \sin\theta \, d\theta} = -\frac{N_0}{E_n}.$$

Thus the recoil protons from a monoenergetic beam of neutrons are evenly distributed in energy from zero energy up to the energy of the neutrons. Figure 4A illustrates the distribution in energy of recoil protons from monoenergetic neutrons. Now if there is a second group of monoenergetic lower energy neutrons also present, the distribution would be of the nature as shown in Figure 4B. Since it is impossible experimentally to obtain completely monoenergetic neutrons,

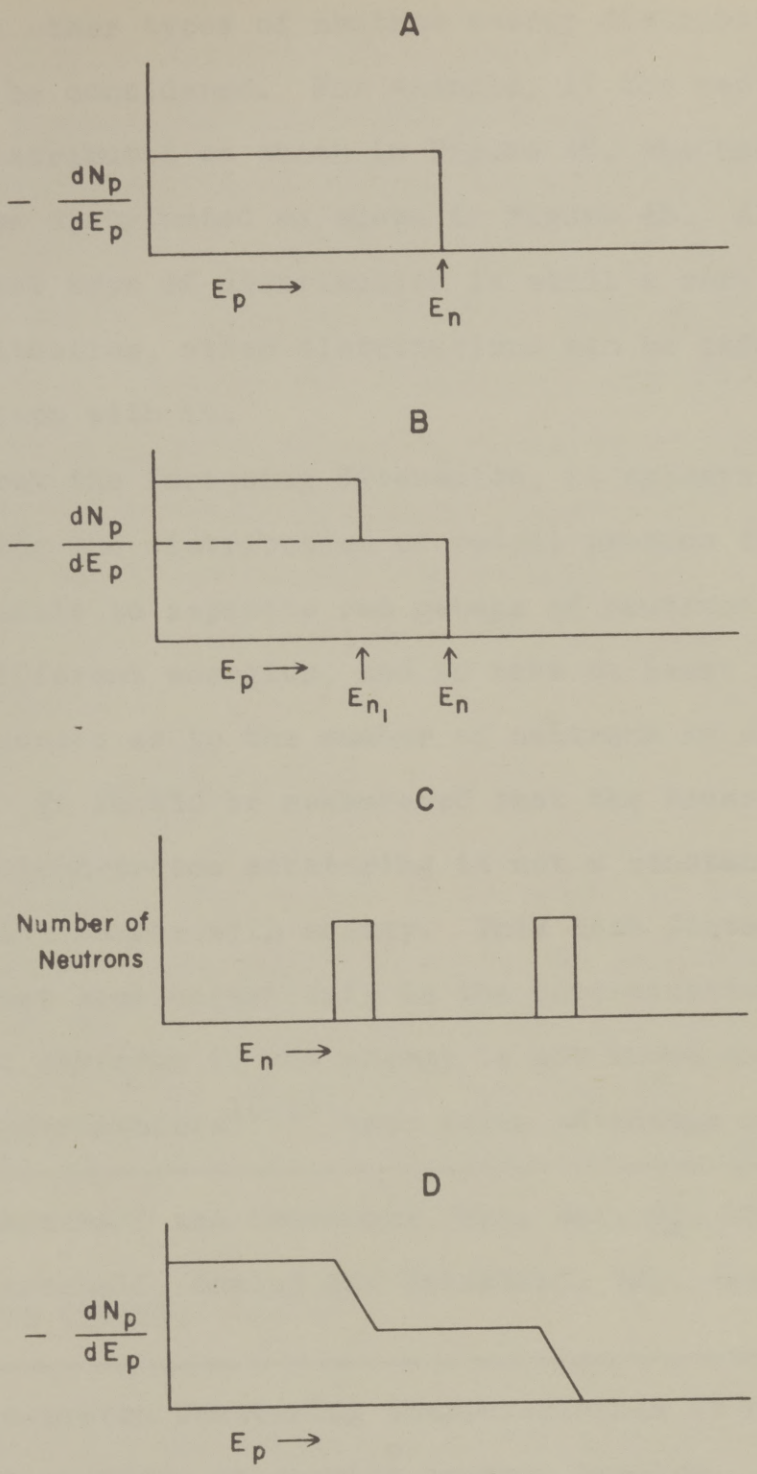

FIGURE 4. IDEALIZED PROTON RECOIL DISTRIBUTIONS

certain other types of neutron energy distribution should be considered. For example, if the neutrons were distributed as shown in Figure 4C, the protons would be distributed as shown in Figure 4D. Although this last type of distribution is still a very idealized situation, other distributions can be inferred by comparison with it.

From the foregoing discussion, it appears that by observing the distribution of recoil protons it should be possible to separate out groups of neutrons which have different energies, and to make at least intelligent guesses as to the number of neutrons in each group. It should be remembered that the cross section for neutron-proton scattering is not a constant quantity, but varies with energy. This last factor may introduce some uncertainty in the determination of numbers of neutrons if the energy is not known exactly.

Experimenters[18,19] have taken advantage of the

---

18. Barschall and Ladenburg, Phy. Rev. 61, 129 (1942).

19. Barschall, Manley and Weisskopf, Phy. Rev. 72, 875 (1947).

---

neutron-proton scattering characteristics by using ionization chambers to examine neutron spectra. The disadvantage is that the efficiency of ionization chambers is so low that the time required to obtain reliable data is quite long. On the other hand, the density of

nuclei in a liquid or solid scintillation counter is much greater, and hence the efficiency is considerably higher. This higher efficiency makes experiments feasible which were impractical with ionization chambers.

Figure 2 shows the geometry used with the iron scatterer. A ring type of geometry was chosen to have the maximum number of scattered neutrons for a given scatterer thickness and given geometrical latitude on the angle of scattering for the neutrons.

Differential angular scattering cross section may be defined as

$$\frac{d\sigma(\theta)}{d\omega} = \frac{N(\theta)}{n_1 N_s}$$

where $N(\theta)$ is the number of neutrons per steradian scattered at an angle, θ, n_1 is the number of scattering centers per square centimeter, and N_s is the number of neutrons incident on the scatterer. In order to use this formula, it is necessary to express it in terms of the parameters of the experiment. Now

$$N(\theta) = \frac{\delta I \, R^2}{c \, A_d}$$

where: c = the efficiency of the counter

δI = the number of counts from scattered neutrons

R = the distance from the scatterer to the detector

A_d = the area of the detector.

N_s should be the average number of neutrons falling on the scatterer. Since the scatterer is not infinitely thin, a correction must be made for the neutrons which are scattered out of the neutron beam. The number, N, of neutrons at a depth, x, of the scatterer is given by $N = N_0 e^{-n\sigma_t x}$ where N_0 is the number of neutrons incident on the surface of the scatterer, n is the number of scattering centers/cm.^{3} and σ_t is the total cross section for the scattering material. Thus the average number of neutrons in the scatter, N_s, is given by

$$N_s = \bar{N} = \frac{1}{a} \int_0^a N_0 \, e^{-n\sigma_t x} \, dx$$

$$= \frac{N_0}{n\sigma_t a} (1 - e^{-n\sigma_t a})$$

where a is the total thickness of the scatterer or, since $na = n_1$

$$N_s = \frac{N_0}{n_1 \sigma_t} (1 - e^{-n\sigma_t a}).$$

Expressing N_0 in terms of the counting rate of the detector gives

$$N_0 = \frac{f I_0 A_s d_4^2}{c A_d r_1^2}$$

where: A_s = the area of the scatterer subtended at the target

d_4 = the distance from the target to the detector

r_1 = the distance from the target to the scatterer

I_0 = the counting rate of the detector due to the direct beam of neutrons from the target

f = a numerical factor to account for the difference in the intensity of the beam of neutrons at the scatterer angle and the intensity of the beam in the forward direction. This difference occurs because of the angular asymmetry of the neutron distribution from the target.

The formula for differential angular scattering cross section then becomes[20,21]

$$\frac{d\sigma(\theta)}{d\omega} = \frac{\sigma_t R^2 r_1^2 \delta I}{f A_s d_4^2 (1 - e^{-n\sigma_t a})} .$$

---

20. Barschall and Ladenburg, op cit.

21. Leonard, B. P., "The Differential Angular Scattering of Neutrons from Aluminum and Copper", Ph. D. Dissertation, University of Texas, May, 1953 (to be published).

For a given position of the scatterer, this can be simplified to

$$\frac{d\sigma(\theta)}{d\omega} = K \frac{R^2 \delta I}{d_4^2 I_0}$$

The values of K used in the calculations are listed in the data tables.

The procedure in measuring inelastic cross section is first to measure the differential angular scattering with a high value of the discriminator voltage, E, where the dominant factor in the counting rate is the elastically scattered neutrons, and then to measure the differential angular scattering at a low value of the discriminator voltage, E, where the counting rate is due to both elastically scattered and inelastically scattered neutrons. The difference in cross sections should be corrected for the change in neutron-proton cross section since the lower energy neutrons have a higher probability of collision with protons.

Figure 5 shows the discriminator spectrum obtained when the counter is exposed to the direct beam of neutrons from the target. The discriminator voltages are expressed in terms of divisions of the E dial. If conversion to voltage is desired, 1500 divisions of E equals 80 volts. This discriminator spectrum corre-

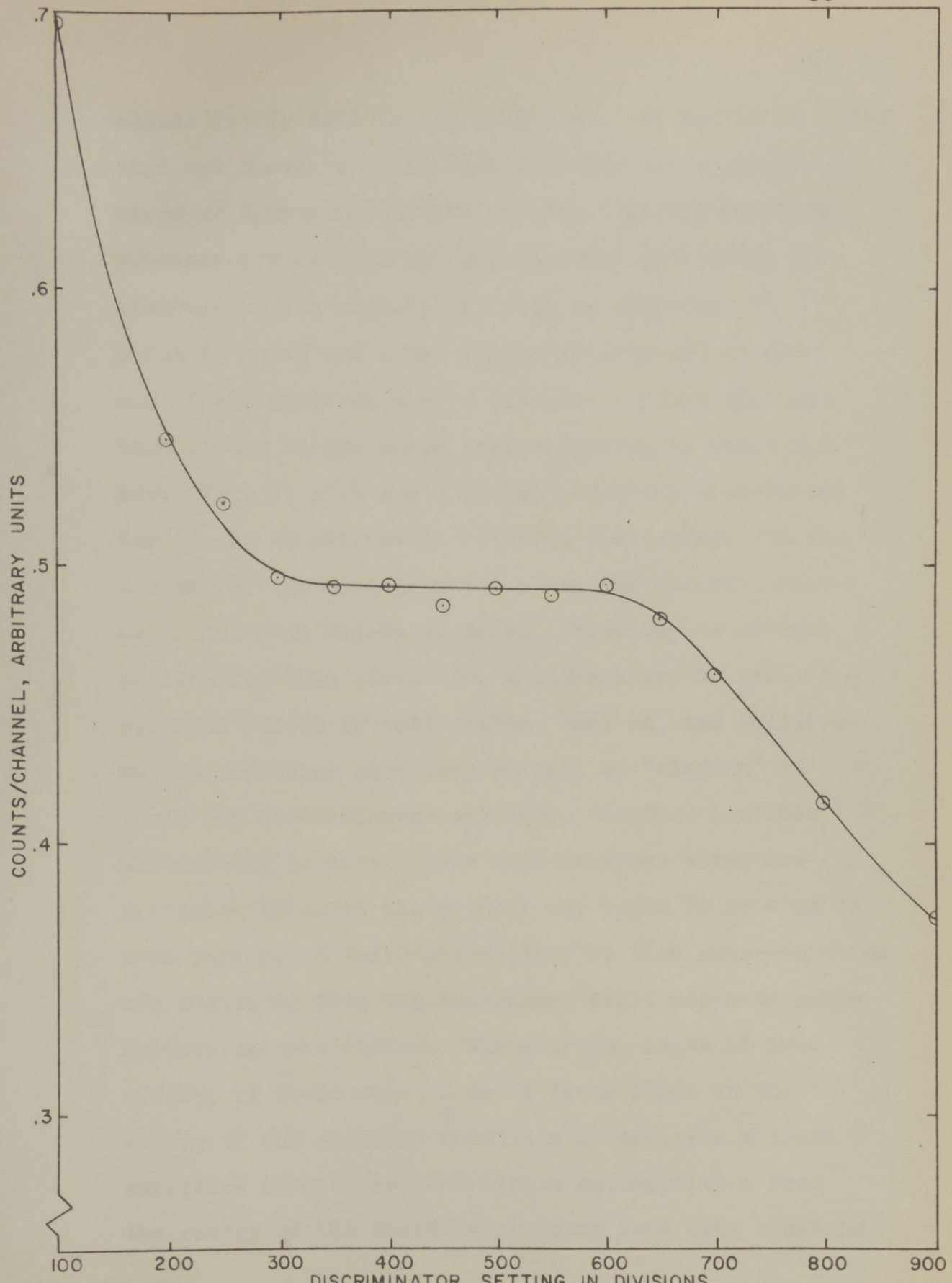

FIGURE 5. DISCRIMINATOR SPECTRUM OF DIRECT BEAM

sponds fairly well to the predicted. It should be noted that the curve is quite flat between discriminator settings of approximately 650 and 250. At discriminator voltages higher than 650 the counting rate drops off, although not as rapidly as might be desired. The point at which the curve begins to drop off at this end of the spectrum can be taken as a rough calibration of the energy scale, corresponding to about 2.8 mev. This is also the point at which the discriminator is set to measure the elastic scattering. On the low end of the discriminator curve the counting rate begins to rise fairly rapidly. There may be several reasons for this rise. The equipment may be producing spurious pulses in this region, that is, the amplifier may be producing secondary pulses, or "ringing" at these low discriminator settings. Another possible explanation is that pulses from neutrons which are scattered twice in the counter may begin to show up in this region. A third possibility is that neutrons which are scattered from the laboratory walls may have pulse heights in this region. Whatever the cause of the effect, it would seem to set a lower limit on the energy of the neutrons which can be detected without sacrifice of accuracy. A linear extrapolation from the energy of the incident neutrons sets this limit in

the region between 0.5 and 1.0 mev. It may be possible to lower this limit slightly, but since the amplifier is non-linear for pulses which are larger than about 1050 divisions on the discriminator, increasing the amplifier gain would tend to destroy the accuracy on the high end of the discriminator.

Figure 6 and Figure 7 show the discriminator spectrum of the scattered neutrons. Figure 6 shows data obtained without the use of an attenuator, and Figure 7 shows data taken with an attenuator. The general shapes of the curves are the same, although the data taken with an attenuator seems to show more detail than the data taken without an attenuator. This can be accounted for by the higher statistical accuracy obtained with the attenuator. There is a very definite break in the curve at a discriminator setting of approximately 300. It is believed that the variations from a smooth curve are actually due to the appearance of the inelastically scattered neutrons from the different levels of the residual iron nucleus. The appearance of these breaks mark places which should be investigated by the angular scattering method. These breaks, then, are the deciding factor in setting the discriminator bias for measuring inelastic scattering.

For each inelastically scattered neutron there

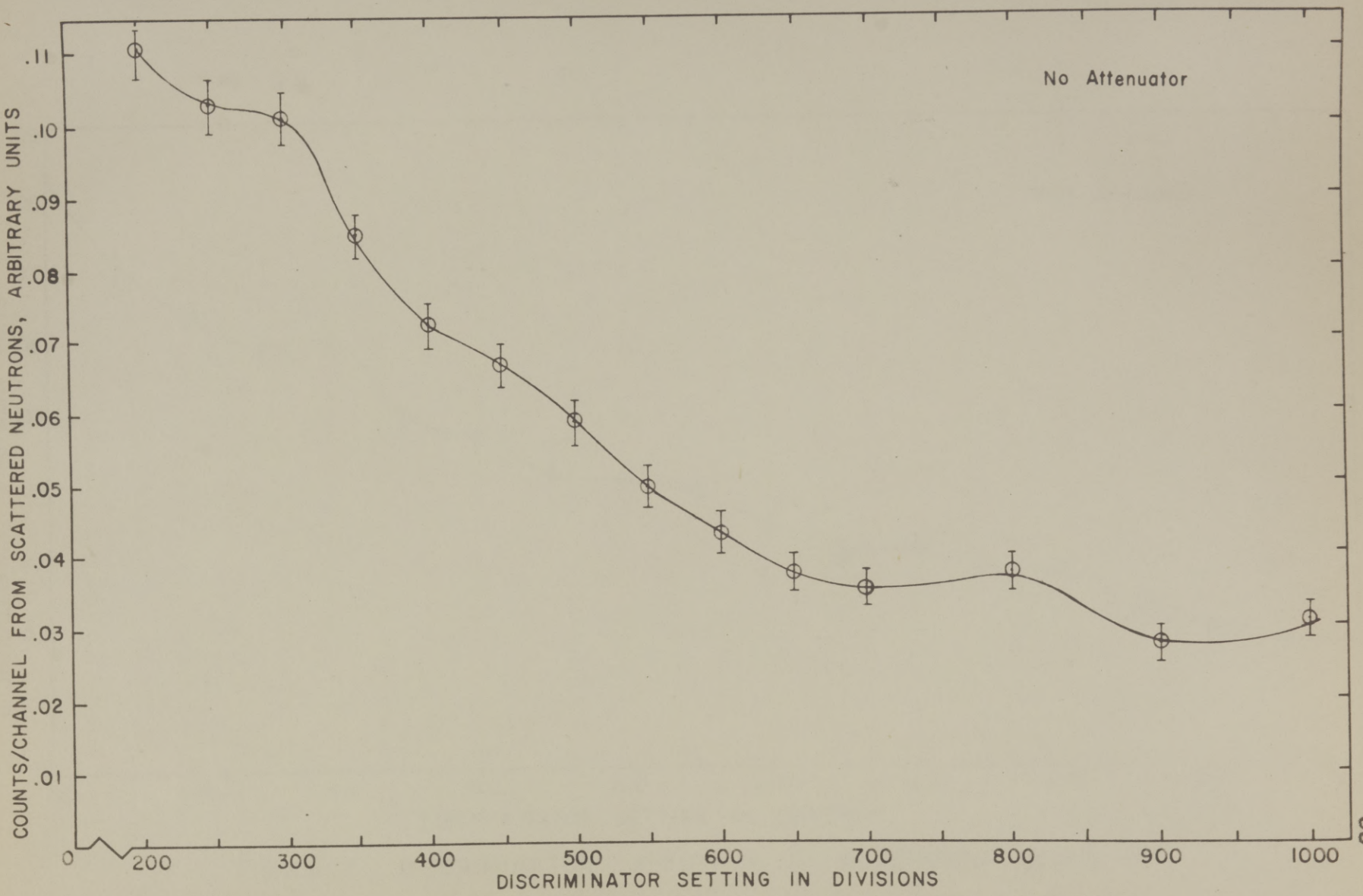

FIGURE 6. DISCRIMINATOR SPECTRUM OF SCATTERED NEUTRONS

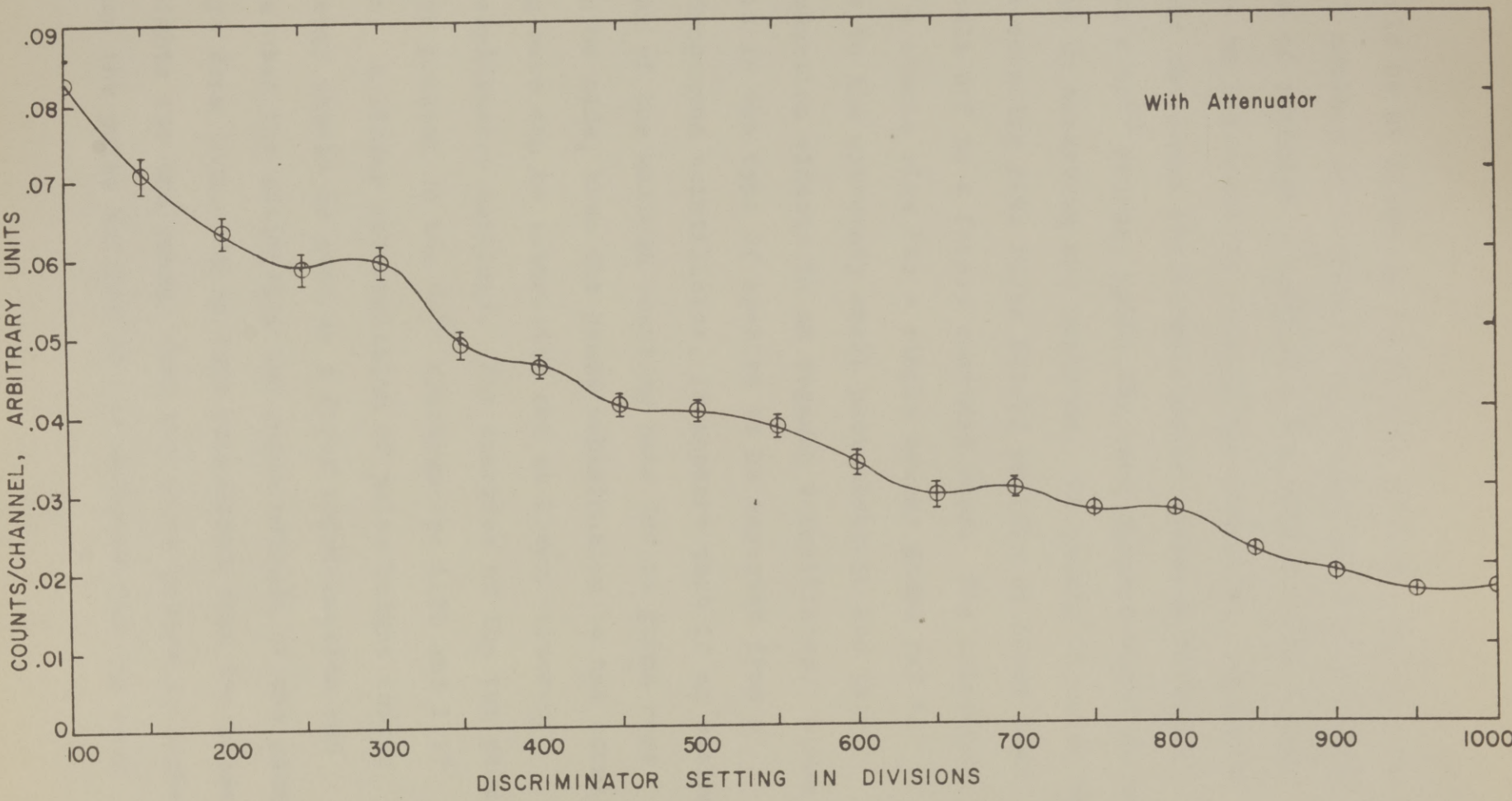

FIGURE 7. DISCRIMINATOR SPECTRUM OF SCATTERED NEUTRONS

should be at least one gamma ray emitted from the residual nucleus as it decays to the ground state. It is thus of interest to estimate the effect of the gamma rays on the counting rate of the detector. Figure 8 shows the gamma ray discriminator spectrum obtained from a Co^{60} source, using the same channel width as was used in observing the neutrons. It should be noted that the counting rate rises fairly rapidly at first then levels off to a fairly constant rate. The occurence of a single rise for a single energy gamma ray is due to the extremely small photoelectric and pair production effects in an organic scintillator. Since this is the type of spectra to be expected from a hydrogenous scintillator, it appears that if an estimation of the maximum counting rate due to gamma rays can be made, then the gamma contribution to the counting rate can be subtracted out at lower values of discriminator settings. The energies of the two gamma rays present in the Co^{60} spectrum are 1.33 and 1.17 mev. A linear extrapolation of pulse height versus energy should be good as a first approximation and was used for estimating the pulse heights of the gamma rays from iron. It is very convenient that the pulse heights for the gammas turn out to be generally higher than the pulse heights of the neutrons for the same

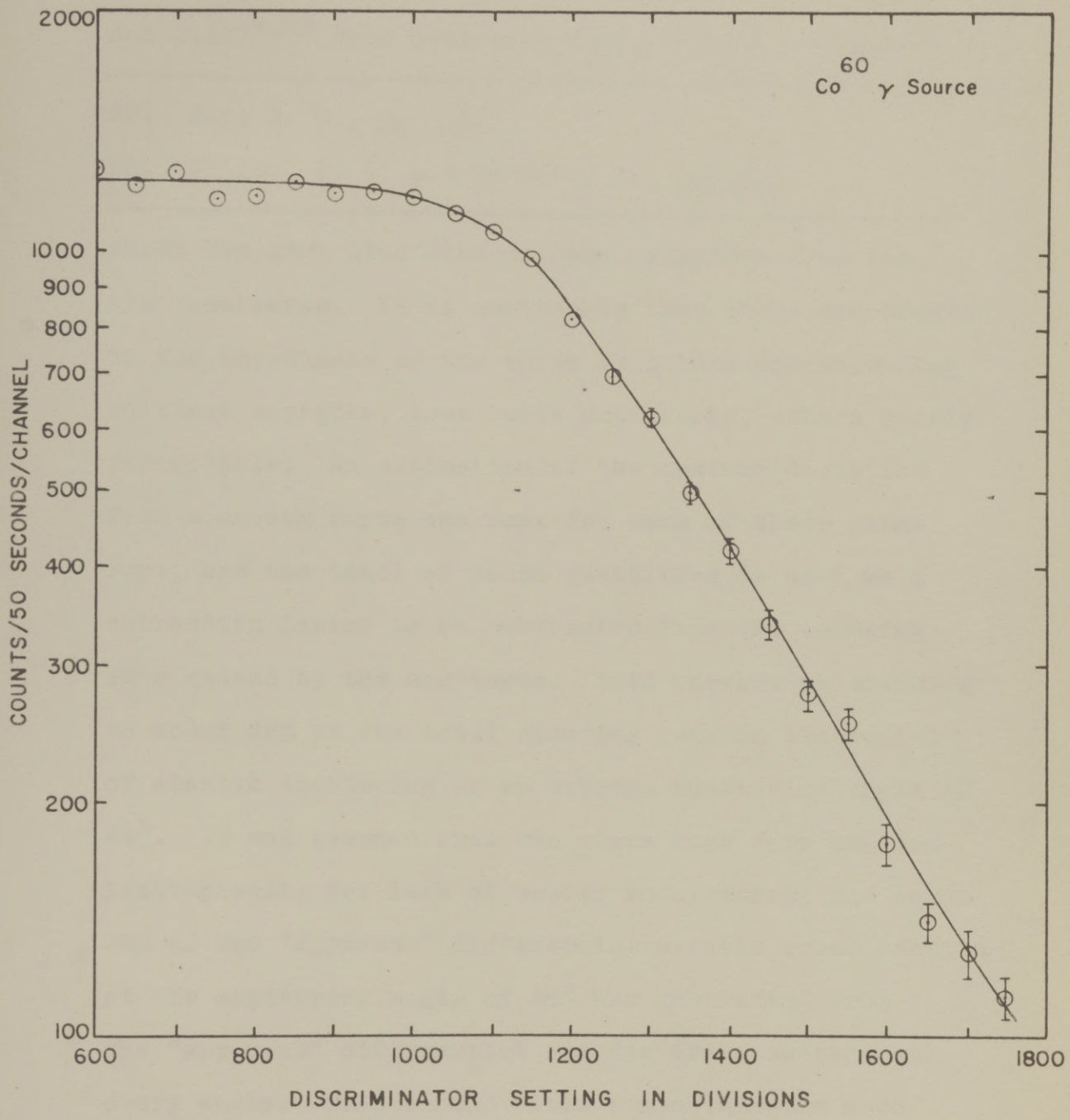

FIGURE 8. DISCRIMINATOR SPECTRUM OF Co^{60} γ RAYS

energy.

Gamma rays of energies 0.845, 1.24, 1.42, 1.80 and 2.13[22,23] have been reported for iron. Figure 9

---

22. Day, R. B., op cit.

23. Elliot, L. G. and Deutsch, M., op cit.

---

shows the high bias discriminator spectrum from the iron scatterer. It is noticeable that there are breaks in the smoothness of the curve at points corresponding to these energies, some quite noticeable, others barely perceptible. An estimation of the maximum deviation from a smooth curve was made for each of these gamma rays, and the total of these quantities is used as a correction factor to be subtracted from the counting rate caused by the scatterer. This correction amounted to about 22% of the total counting rate in the region of elastic scattering at an average scattering angle of 44°. It was assumed that the gamma rays were emitted isotropically for lack of better information, and hence 22% of the "apparent" differential elastic cross section at the scattering angle of 44° was subtracted from the "apparent" differential elastic cross section at every angle. This should yield a considerably more accurate value of the differential elastic cross section. Since there were no gamma rays appearing in the

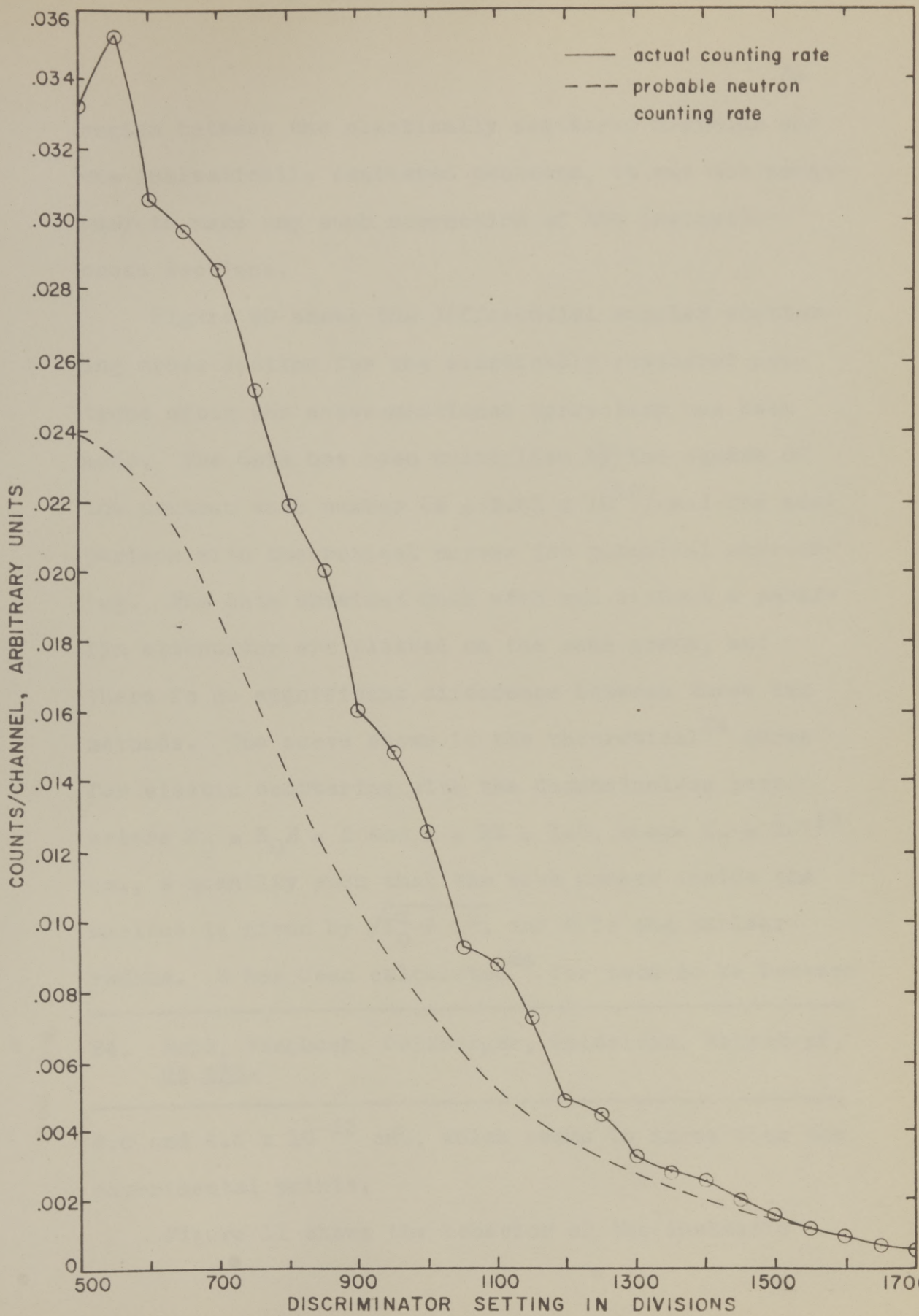

FIGURE 9. HIGH BIAS DISCRIMINATOR SPECTRUM OF SCATTERED NEUTRONS

region between the elastically scattered neutrons and the inelastically scattered neutrons, it was not necessary to make any such correction of the inelastic cross sections.

Figure 10 shows the differential angular scattering cross section for the elastically scattered neutrons after the above-mentioned correction has been made. The data has been multiplied by the square of the neutron wave number ($k = 3.61 \times 10^{12}$/cm.) for comparison with theoretical curves for potential scattering. The data obtained both with and without a paraffin attenuator are plotted on the same graph, and there is no significant difference between these two methods. The curve shown is the theoretical[24] curve for elastic scattering with the dimensionless parameters $X_0 = K_0R = 5$ and $x = kR = 1.7$, where $K_0 = 10^{-13}$ cm., a quantity such that the wave number inside the nucleus is given by $\sqrt{K_0^2 + k^2}$, and R is the nuclear radius. R has been calculated[24] for iron to be between

---

24. Feld, Feshbach, Goldberger, Goldstein, Weisskopf, op cit.

4.0 and 4.6×10^{-13} cm., which seems to agree with the experimental points.

Figure 11 shows the behavior of the inelastic

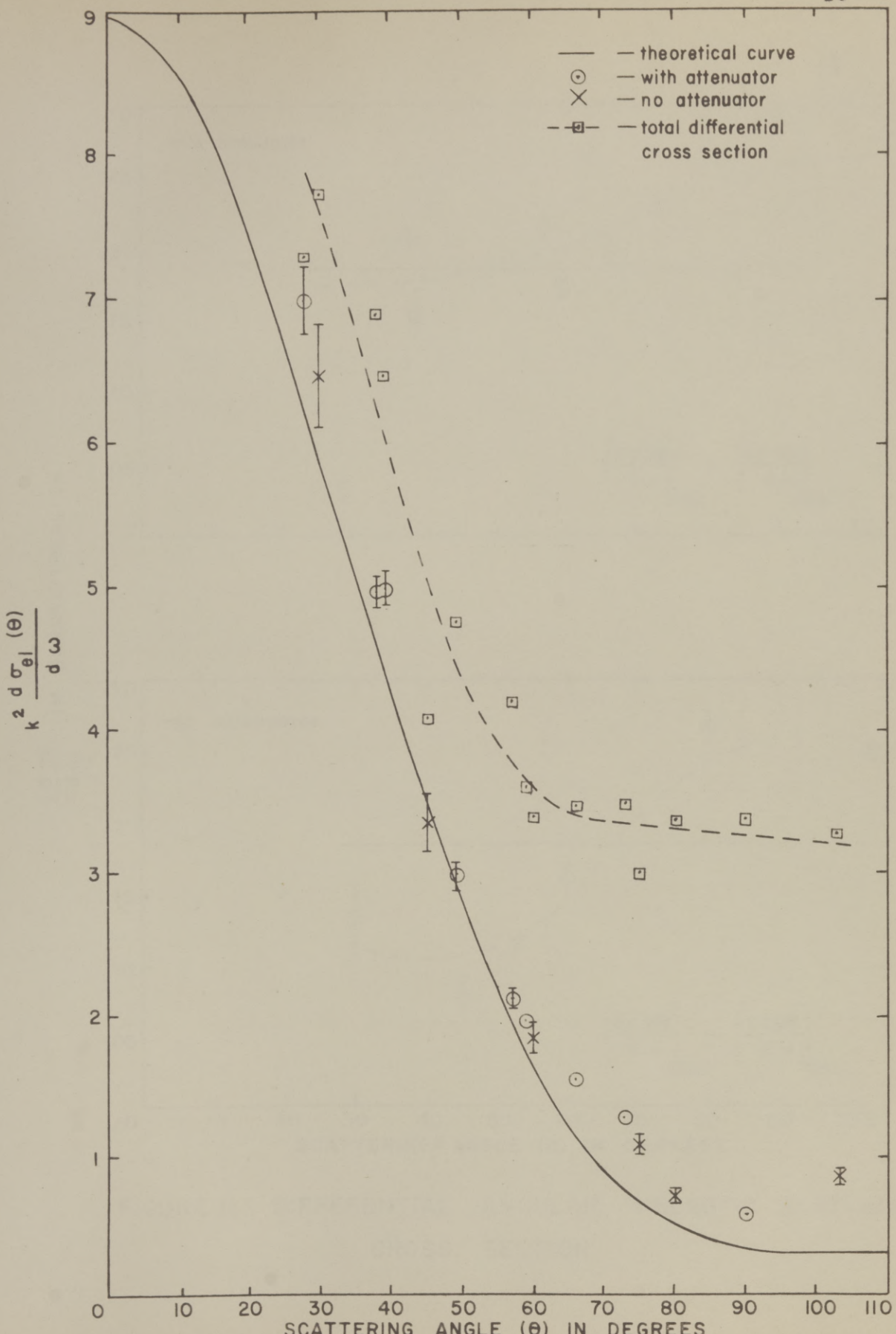

FIGURE 10. DIFFERENTIAL ANGULAR ELASTIC SCATTERING CROSS SECTION

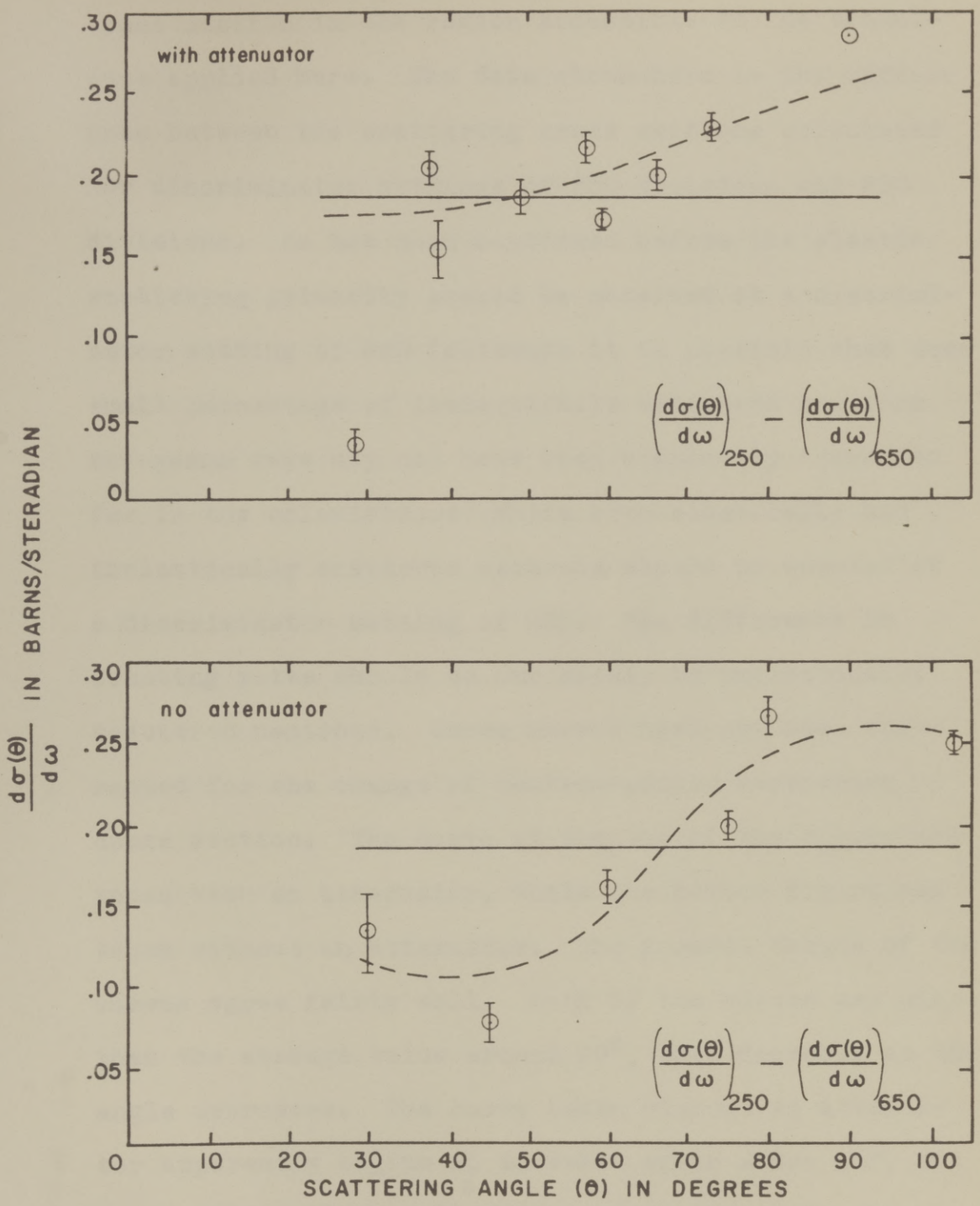

FIGURE II. DIFFERENTIAL ANGULAR INELASTIC SCATTERING CROSS SECTION

cross section in the region accessible to the techniques applied here. The data shown here is the difference between the scattering cross sections calculated for discriminator settings of 250 divisions and 650 divisions. As has been mentioned before the elastic scattering primarily should be observed at a discriminator setting of 650 (although it is possible that some small percentage of inelastically scattered neutrons and gamma rays may not have been completely corrected for in the calculations) while both elastically and inelastically scattered neutrons should be counted at a discriminator setting of 250. The difference in counting rates should be due solely to inelastically scattered neutrons. These curves have not been corrected for the change of neutron-proton scattering cross section. The curve at the top of the figure was taken with an attenuator, while the bottom figure was taken without an attenuator. The general shapes of the curves agree fairly well. Both of the curves are higher than the average value around 90°, then decrease as the angle decreases. The curve taken without an attenuator apparently begins to increase again after 45°, but it is difficult to tell whether the curve with the attenuator should do the same thing or not. A straight line has been drawn through the mean of the points of

both curves to indicate deviations from this mean. Dotted curves have been drawn to indicate the probable shape of the curves.

Figure 12 represents an attempt to subdivide the inelastic scattering into groups corresponding to the energy levels. This set of data was taken with an attenuator, but the statistics still leave considerable room for improvement. The best guess at the shape of an individual curve is probably a straight line. There is some evidence again of a consistent trend for the points at 90° to be higher than the average. Of course, trends which do not show up on the individual curves may show up on the composite curve which is plotted in Figure 11. Possibly counting times of the order of ten to one hundred times as long as the ones used or higher fluxes of neutrons might show up enough detail on these individual curves to warrant further conclusions to be drawn from them.

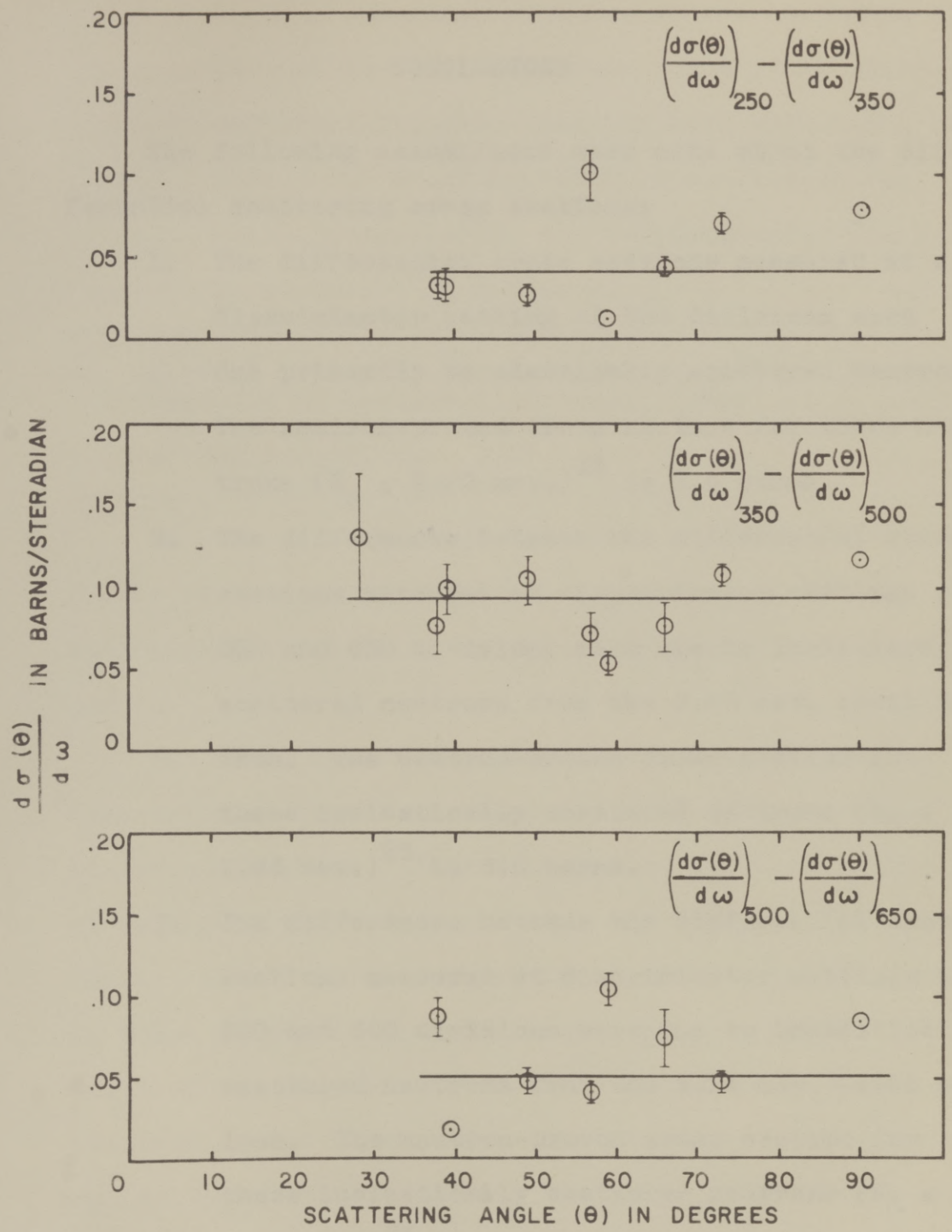

FIGURE 12. COMPONENTS OF DIFFERENTIAL ANGULAR INELASTIC SCATTERING CROSS SECTION

CHAPTER VI

CONCLUSIONS

The following assumptions were made about the differential scattering cross sections:

1. The differential cross sections measured at a discriminator setting of 650 divisions were due primarily to elastically scattered neutrons. The neutron-proton cross section for these neutrons (E_n = 2.80 mev.)[25] is 2.4 barns.
2. The differences between the differential cross sections measured at discriminator settings of 500 and 650 divisions were due to inelastically scattered neutrons from the 0.85 mev. level of iron. The neutron-proton cross section for these inelastically scattered neutrons (E_n = 1.95 mev.)[25] is 3.0 barns.
3. The differences between the differential cross sections measured at discriminator settings of 350 and 500 divisions were due to inelastically scattered neutrons from the 1.24 mev. level of iron. The neutron-proton cross section for these inelastically scattered neutrons (E_n = 1.56 mev.)[25] is 3.3 barns.
4. The differences between the differential cross

sections measured at discriminator settings of 250 and 350 divisions were due to inelastically scattered neutrons from the 1.42 mev. level of iron. The neutron-proton cross section for these inelastically scattered neutrons (E_n = 1.38 mev.)[25] is 3.5 barns.

25. Allred, J. C. and Armstrong, A. H., "Laboratory Handbook of Nuclear Microscopy (Tentative)", Los Alamos Scientific Laboratory of the University of California, Nov. 1951.

An average neutron-proton cross section correction factor of 0.74 is used on the curves for the total inelastically scattered neutrons, that is, the 250-650 curves.

The total inelastic scattering cross section is then calculated on the assumption of isotropy of the scattered neutrons. This calculation consists simply of multiplying the average value of the differential angular cross section, which is in barns/steradian, by 4π which is the total solid angle about a point. A value of the inelastic cross section of 1.7 barns is obtained in this manner for the data taken both with and without the attenuator. The value of 1.7 barns agrees quite favorably with the values of Barschall and Ladenburg[26] which vary between the limits of 1.4

26. Barschall and Ladenburg, op cit.

and 2.6 barns at a neutron energy of 2.5 mev. This value is somewhat higher than the value of 1.1 barns given by Barschall, et al.[27] from a "poor geometry"

27. Barschall, Manley and Weisskopf, op cit.

experiment at a neutron energy of 3.1 mev. An approximate integration of the elastic scattering yields a value of 1.6 barns for this cross section, which gives a total scattering cross section of 3.3 barns, which is in good agreement with the accepted value of 3.2 barns.[28]

28. Miller, D. W., Adair, R. K., Bockelman, C. K., Dardes, S. F., Phy. Rev. 88, 83 (1952).

It is somewhat difficult to estimate the probable error in the experiment. The averages of the experimental points for inelastic scattering with and without the attenuator are the same. The sum of the total elastic and the total inelastic cross sections differs by 3% from the accepted value of the total cross section. The assumption of slightly different functional forms for the angular variations of the cross sections may yield as much as ±5% variation in the total cross section value. Small errors in measurements of distances may also contribute to the error. Considering

these various factors, it is believed that the error is not greater than ±10% of the values measured.

Both graphs in Figure 11 indicate an anisotropy in the inelastic scattering. Unfortunately it was impossible to check the scattering at angles smaller than 30° and at angles larger than 105° with the scatterer used. Both the angular distributions measured are in fair agreement with an assumption of an angular distribution function of the form

$$\sigma(\theta) = A_0 + A_1 \cos^2\theta$$

while the angular distribution measured without the attenuator could also be fitted to an angular distribution of the form

$$\sigma(\theta) = B_0 + B_1 \cos^2\theta + B_2 \cos^4\theta.$$

Either of these distribution functions might be expected from the predictions of Feld, et al.[29]

---

29. Feld, Feshbach, Goldberger, Goldstein, Weisskopf, op cit.

The method used here to obtain differential inelastic cross section has been shown to be feasible. The lower energy limit on the neutrons which can be measured is of the same order of magnitude as that of photographic plates. A slightly lower energy limit can be

obtained with an ionization chamber although this limit is still about the same order of magnitude. The principal objection to ionization chambers and photographic plates is the length of time necessary to obtain data which is statistically reliable.

One factor which is present in the scintillation counter, which is not present in other methods, is the attenuation of light pulses originating in the scintillator volume farthest from the photocathode. This effect probably accounts for the absence of a very sharp break in the counting rate as a function of the discriminator, since this attenuation will tend to smear out the energy resolution of the counter. This difficulty could be evaded to some extent by making the scintillating volume thinner, although decreasing the volume will lower the efficiency of the counter. Some further improvement might also be gained by careful selection of the 5819 photomultiplier tubes for best linearity of pulse response to light pulses. It may be that scintillators other than terphenyl (such as anthracene) might give better resolution. The modifications given above coupled with longer counting time should improve the results to some extent, but the present results appear to be reliable.

CHAPTER VII

DATA TABLES

SYMBOLS USED IN DATA TABLES

d_1 = distance from target to bottom of scatterer.

d_2 = distance from target to top of counter.

d_3 = distance from target to middle of scatterer.

d_4 = distance from target to middle of counter.

R = distance from center of scatterer to center of counter.

θ = average scattering angle.

E = position of discriminator dial.

ΔE = position of window width dial.

I_0 = $\frac{\text{detector counts-background}}{\text{monitor counts-background}}$ with no scatterer present.

ΔI = ratio of detector counts to monitor counts with scatterer in minus ratio of detector counts to monitor counts with scatterer out.

TABLE I

Monitor Background = 1749/300 seconds d_1 = 28.0 cm. d_4 = 26.4 cm.

ΔE = 556 = 50 Divisions of E d_2 = 23.5 cm. R^2 = 34.93 cm^2

No Attenuator d_3 = 26.7 cm. $\theta = 106^\circ$

Time in Sec.	E Div.	Scatterer	Monitor Counts - Background	Detector Counts - Background	$\frac{\text{Detector-Background}}{\text{Monitor-Background}}$	δI
300	100	In	64,356	53,826	.9879 ± .0039	
300	100	Out	70,696	49,198	.6959 ± .0028	.2920 ± .0048
300	200	In	67,472	44,237	.6556 ± .0028	
300	200	Out	67,996	37.082	.5454 ± .0024	.1102 ± .0037
300	250	In	70,915	44,381	.6258 ± .0026	
300	250	Out	68,065	35,586	.5228 ± .0024	.1030 ± .0035
300	300	In	70,388	41,977	.5964 ± .0025	
300	300	Out	67,356	33,369	.4954 ± .0023	.1010 ± .0034
300	350	In	69,915	40,364	.5773 ± .0024	
300	350	Out	69,755	34,371	.4927 ± .0022	.0846 ± .0033
300	400	In	70,679	39,929	.5649 ± .0024	
300	400	Out	65,786	32,424	.4929 ± .0023	.0720 ± .0033
300	450	In	72,628	40,089	.5520 ± .0023	
300	450	Out	70,025	33,992	.4854 ± .0022	.0666 ± .0033
300	500	In	74,147	40,824	.5506 ± .0023	
300	500	Out	66,078	32,521	.4922 ± .0023	.0584 ± .0033

TABLE I (continued)

Time in Sec.	E Div.	Scat-terer	Monitor Counts - Background	Detector Counts - Background	$\frac{\text{Detector-Background}}{\text{Monitor-Background}}$	δI
300	550	In	69,987	37,690	.5385 ± .0023	
300	550	Out	70,310	34,394	.4892 ± .0022	.0493 ± .0033
300	600	In	71,263	38,221	.5363 ± .0023	
300	600	Out	68,055	33,571	.4933 ± .0022	.0430 ± .0033
300	650	In	71,755	37,164	.5179 ± .0022	
300	650	Out	71,042	34,113	.4802 ± .0022	.0377 ± .0031
300	700	In	71,717	35,562	.4959 ± .0022	
300	700	Out	64,022	29,466	.4602 ± .0022	.0357 ± .0031
300	800	In	69,414	31,318	.4512 ± .0021	
300	800	Out	65,078	26,944	.4140 ± .0020	.0372 ± .0030
300	900	In	71,477	28,534	.3992 ± .0019	
300	900	Out	64,721	24,045	.3715 ± .0019	.0277 ± .0027
300	1000	In	69,718	23,694	.3399 ± .0017	
300	1000	Out	67.003	20,705	.3090 ± .0017	.0309 ± .0024

TABLE II

Monitor Background = 1786/300 seconds | d_1 = 28.3 cm. | d_4 = 31.0 cm.

ΔE = 556 = 50 Divisions of E | d_2 = 28.1 cm. | R^2 = 54.70 $cm.^2$

With Attenuator | d_3 = 26.5 cm. | $\theta = 65^\circ$

Time in Sec.	E Div.	Scat-terer	Monitor Counts -Background	Detector Counts -Background	$\frac{\text{Detector-Background}}{\text{Monitor-Background}}$	δI
300	50	In	13,439	3,666	.2728 ± .0034	
300	50	Out	14,140	2,145	.1517 ± .0024	.1211 ± .0042
300	100	In	13,343	2,318	.1737 ± .0027	
300	100	Out	22,612	2,064	.0913 ± .0016	.0824 ± .0032
300	150	In	15,786	2,231	.1413 ± .0022	
300	150	Out	28,937	2,044	.0706 ± .0011	.0707 ± .0025
300	200	In	18,937	2,353	.1243 ± .0019	
300	200	Out	35,492	2,159	.0608 ± .0010	.0635 ± .0022
300	250	In	18,332	2,099	.1145 ± .0018	
300	250	Out	41,202	2,310	.0561 ± .0009	.0584 ± .0021
300	300	In	21,169	2,325	.1098 ± .0017	
300	300	Out	41,408	2,080	.0502 ± .0008	.0596 ± .0019
300	350	In	21,726	2,090	.0962 ± .0015	
300	350	Out	40,233	1,906	.0474 ± .0008	.0488 ± .0017
300	400	In	22,319	2,045	.0916 ± .0015	
300	400	Out	39,448	1,799	.0456 ± .0008	.0460 ± .0017

TABLE II (continued)

Time in Sec.	E Div.	Scat-terer	Monitor Counts -Background	Detector Counts -Background	Detector-Background / Monitor-Background	δ I
300	450	In	24,686	1,998	.0809 ± .0013	
300	450	Out	39,633	1,580	.0399 ± .0007	.0410 ± .0015
300	500	In	27,116	2,084	.0769 ± .0012	
300	500	Out	39,643	1,464	.0369 ± .0007	.0400 ± .0014
300	550	In	27,943	2,059	.0737 ± .0012	
300	550	Out	38,683	1,375	.0355 ± .0007	.0382 ± .0014
300	600	In	28,964	1,939	.0669 ± .0011	
300	600	Out	38,115	1,290	.0338 ± .0007	.0331 ± .0013
300	650	In	33,924	2,115	.0623 ± .0010	
300	650	Out	38,323	1,255	.0327 ± .0007	.0296 ± .0012
300	700	In	34,021	1,987	.0584 ± .0010	
300	700	Out	37,900	1,078	.0284 ± .0006	.0300 ± .0012
300	750	In	38,037	2,125	.0559 ± .0009	
300	750	Out	37,994	1,083	.0285 ± .0006	.0274 ± .0011
300	800	In	43,822	2,298	.0524 ± .0008	
300	800	Out	38,525	972	.0252 ± .0006	.0272 ± .0010
300	850	In	42,999	1,996	.0464 ± .0007	
300	850	Out	37,333	911	.0244 ± .0006	.0220 ± .0010

TABLE II (continued)

Time in Sec.	E Div.	Scat-terer	Monitor Counts -Background	Detector Counts -Background	Detector-Background / Monitor-Background	δI
300	900	In	42,840	1,810	.0423 ± .0007	
300	900	Out	37,380	881	.0236 ± .0006	.0187 ± .0010
300	950	In	43,035	1,603	.0372 ± .0005	
300	950	Out	38,014	777	.0204 ± .0005	.0168 ± .0008
300	1000	In	42,742	1,560	.0365 ± .0005	
300	1000	Out	38,217	735	.0192 ± .0005	.0173 ± .0008

TABLE III*

Co^{60} source--1 meter from counter

$\Delta E = 278 = 25$ divisions of E

*Note: Table III was taken with an amplifier gain $\frac{1}{2}$ as much as Tables I, II, V, and VI.

Time in Sec.	E in Divisions	Counts
50	200	1526 ± 26
50	225	1383 ± 25
50	250	1306 ± 24
50	275	1321 ± 25
50	300	1276 ± 24
50	325	1205 ± 23
50	350	1257 ± 24
50	375	1164 ± 23
50	400	1178 ± 23
50	425	1225 ± 24
50	450	1187 ± 23
50	475	1194 ± 24
50	500	1176 ± 23
50	525	1119 ± 23
50	550	1065 ± 22
50	575	982 ± 21
50	600	829 ± 19
50	625	700 ± 18

TABLE III (continued)

Time in Sec.	E in Divisions	Counts
50	650	620 ± 17
50	675	501 ± 15
50	700	421 ± 14
50	725	339 ± 12
50	750	277 ± 11
50	775	253 ± 11
50	800	179 ± 9
50	825	142 ± 8
50	850	128 ± 8
50	875	114 ± 7
50	900	96 ± 7
50	925	86 ± 6
50	950	78 ± 6
50	975	60 ± 5
50	1000	47 ± 5
50	1025	31 ± 4
50	1050	22 ± 3

TABLE IV*

ΔE = 278 = 25 Divisions of E

With Attenuator

d_1 = 26.5 cm. d_4 = 34.9 cm.

d_2 = 32.0 cm. R^2 = 138.04 $cm.^2$

d_3 = 24.7 cm. θ = 44°

* Note: Table IV was taken with an amplifier gain $\frac{1}{2}$ as much as Tables I, II, V, and VI.

Time in Sec.	E Div.	Scat-terer	Monitor Counts -Background	Detector Counts -Background	Detector-Background / Monitor-Background	δI
500	250	Bkg.	2,876	201		
600	250	In	95,415	6,806	.07133	
900	250	Out	211,181	8,052	.03813	.03320 ± .00068
500	275	Bkg.	2,791	177		
600	275	In	127,806	9,181	.07184	
900	275	Out	188,948	6,906	.03655	.03529 ± .00064
500	300	Bkg.	2,709	152		
600	300	In	125,876	8,114	.06446	
900	300	Out	186,954	6,320	.03381	.03065 ± .00061
504	325	Bkg.	2,849	119		
600	325	In	123,622	7,557	.06113	
900	325	Out	183,523	5,756	.03136	.02977 ± .00060
500	350	Bkg.	2,851	128		
600	350	In	124,561	7,037	.05649	
905	350	Out	186,040	5,179	.02784	.02865 ± .00056

TABLE IV (continued)

Time in Sec.	E Div.	Scat-terer	Monitor Counts -Background	Detector Counts -Background	Detector-Background / Monitor-Background	δI
500	375	Bkg.	2,753	144		
800	375	In	151,872	7,701	.05071	
1000	375	Out	196,618	5,012	.02549	.02522 ± .00050
500	400	Bkg.	2,953	132		
900	400	In	187,096	8,551	.04570	
1200	400	Out	239,902	5,710	.02380	.02190 ± .00040
500	425	Bkg.	2,907	101		
900	425	In	211,182	8,621	.04082	
1200	425	Out	284,052	5,910	.02081	.02001 ± .00038
500	450	Bkg.	2,885	100		
900	450	In	183,582	6,439	.03507	
1200	450	Out	240,028	4,575	.01904	.01603 ± .00037
500	475	Bkg.	2,889	100		
900	475	In	208,711	6,464	.03097	
1200	475	Out	272,750	4,402	.01614	.01483 ± .00032
500	500	Bkg.	2,887	62		
900	500	In	184,918	4,952	.02678	
1250	500	Out	262,462	3,710	.01414	.01264 ± .00031
500	525	Bkg.	3,019	80		
900	525	In	174,925	3,751	.02144	
1200	525	Out	233,794	2,838	.01214	.00930 ± .00030

TABLE IV (continued)

Time in Sec.	E Div.	Scat-terer	Monitor Counts -Background	Detector Counts -Background	Detector-Background / Monitor-Background	δI
500	550	Bkg.	2,866	97		
1200	550	In	215,355	3,957	.01837	
1200	550	Out	216,565	2,070	.00956	.00881 ± .00026
500	575	Bkg.	2,923	83		
910	575	In	157,114	2,466	.01570	
1200	575	Out	209,324	1,757	.00839	.00731 ± .00026
1000	600	Bkg.	5,894	140		
900	600	In	148,354	1,806	.01217	
1500	600	Out	239,218	1,739	.00727	.00490 ± .00024
500	625	Bkg.	2,925	65		
900	625	In	165,800	1,713	.01033	
1500	625	Out	268,202	1,547	.00577	.00456 ± .00021
1000	650	Bkg.	5,844	145		
4200	650	In	715,977	5,625	.00786	
4800	650	Out	815,309	3,636	.00446	.00340 ± .00012
1000	675	Bkg.	5,836	142		
1400	675	In	242,674	1,698	.00700	
1900	675	Out	320,741	1,321	.00412	.00288 ± .00016
1000	700	Bkg.	5,786	142		
1500	700	In	257,455	1,566	.00608	
2300	700	Out	397,682	1,363	.00343	.00265 ± .00015

TABLE IV (continued)

Time in Sec.	E Div.	Scat-terer	Monitor Counts -Background	Detector Counts -Background	Detector-Background / Monitor-Background	δI
1000	725	Bkg.	5,653	98		
1600	725	In	287,964	1,517	.00527	
2400	725	Out	444,157	1,451	.00327	.00200 ± .00013
1000	750	Bkg.	5,619	103		
2100	750	In	370,533	1,481	.00399	
3200	750	Out	557,533	1,278	.00231	.00168 ± .00011
800	775	Bkg.	4,510	49		
5700	775	In	1,186,947	3,933	.00331	
6300	775	Out	1,278,612	2,683	.00211	.00120 ± .00005
1000	800	Bkg.	5,644	64		
6000	800	In	1,177,405	3,248	.00276	
6000	800	Out	1,172,129	1,970	.00169	.00107 ± .00005
1000	825	Bkg.	5,683	66		
3000	825	In	556,763	1,255	.00225	
3000	825	Out	565,724	852	.00151	.00074 ± .00007
1000	850	Bkg.	5,705	57		
3000	850	In	557,958	1,084	.00194	
3000	850	Out	572,559	732	.00128	.00067 ± .00007

TABLE V

Monitor Background = 1740/300 sec.

ΔE = 525 = 50 Divisions of E

d_1 = 25.0 cm.

d_3 = 23.3 cm.

With Attenuator

R^2 = 627.25 $cm.^2$ $\theta = 28^\circ$

Detector Background (250) = 292/300 sec.

Detector Background (350) = 180/300 sec.

Detector Background (500) = 93/300 sec.

Detector Background (650) = 103/300 sec.

d_2 = 44.7 cm. d_4 = 47.6 cm.

Time in Sec.	E Div.	Scat-terer	Monitor Counts -Background	Detector Counts -Background	$\frac{\text{Detector-Background}}{\text{Monitor-Background}}$	δI
400	250	In	78,154	4,225	.05406	
400	350		78,154	3,372	.04315	
600	650		91,537	2,618	.02860	
600	500		91,537	3,053	.03335	
500	250	Out	76,370	3,015	.03948	.01458 ± .00075
500	350		76,370	2,242	.02936	.01379 ± .00065
600	650		92,246	1,540	.01669	.01191 ± .00048
600	500		92,246	2,051	.02223	.01112 ± .00053
150	250	Out	23,181	4,569	.1971	
150	350	No	23,181	4,126	.1780	
200	650	Atten.	31,372	5,312	.1693	
200	500		31,372	5,567	.1775	

TABLE V (continued)

R^2 = 230.53 cm^2 $\theta = 38^\circ$ d_2 = 34.4 cm. d_4 = 37.3 cm.

Time in Sec.	E Div.	Scat-terer	Monitor Counts -Background	Detector Counts -Background	$\frac{\text{Detector-Background}}{\text{Monitor-Background}}$	δI
800	250	In	129,961	10,553	.08120	
800	350		129,961	8,934	.06874	
800	650		128,360	6,127	.04773	
800	500		128,360	7,461	.05813	
800	250	Out	132,234	6,006	.04542	.03578 ± .00067
800	350		132,234	4,871	.03684	.03190 ± .00061
800	650		130,205	3,231	.02481	.02292 ± .00051
800	500		130,205	3,902	.02997	.02816 ± .00055

TABLE V (continued)

R^2 = 199.68 $cm.^2$ $\theta = 39^\circ$ d_2 = 33.2 cm. d_4 = 36.1 cm.

Time in Sec.	E Div.	Scat-terer	Monitor Counts -Background	Detector Counts -Background	$\frac{\text{Detector-Background}}{\text{Monitor-Background}}$	δI
400	250	In	61,869	5,730	.09262	
400	350		61,869	4,670	.07548	
600	650		90,086	4,874	.05410	
600	500		90,086	5,573	.06186	
600	250	Out	89,329	4,615	.05166	.04096 ± .00133
600	350		89,329	3,499	.03917	.03631 ± .00085
700	650		109,886	2,880	.02621	.02789 ± .00061
700	500		109,886	3,531	.03213	.02973 ± .00067
150	250	Out	24,237	7,812	.3223	
150	350	No	24,237	7,315	.3018	
150	650	Atten.	23,330	6,804	.2916	
150	500		23,330	6,979	.2991	

TABLE V (continued)

R^2 = 107,74 cm^2. θ = 49° d_2 = 28.9 cm. d_4 = 31.8 cm.

Time in Sec.	E Div.	Scat-terer	Monitor Counts -Background	Detector Counts -Background	$\frac{\text{Detector-Background}}{\text{Monitor-Background}}$	δI
300	250	In	47,372	5,672	.11973	
300	350		47,372	4,688	.09896	
500	650		75,856	5,108	.06734	
500	500		75,856	6,031	.07951	
400	250	Out	62,147	3,699	.05952	.06021 ± .00125
400	350		62,147	2,868	.04615	.05281 ± .00118
700	650		107,828	3,503	.03249	.03485 ± .00075
700	500		107,828	4,158	.03856	.04095 ± .00081
200	250	Out	31,329	12,879	.4111	
200	350	No	31,329	11,984	.3825	
200	650	Atten.	30,987	11,705	.3777	
200	500		30,987	11,911	.3844	

TABLE V (continued)

R^2 = 76.28 $cm.^2$ $\theta = 57^\circ$ d_2 = 26,8 cm. d_4 = 29.7 cm.

Time in Sec.	E Div.	Scat-terer	Monitor Counts -Background	Detector Counts -Background	$\frac{\text{Detector-Background}}{\text{Monitor-Background}}$	δ_I
300	250	In	47,294	6,615	.13987	
300	350		47,294	5,019	.10612	
300	650		47,555	3,452	.07259	
300	500		47,555	4,188	.08807	
500	250	Out	82,999	5,290	.06374	.07613 ± .00127
500	350		82,999	4,167	.05021	.05591 ± .00114
500	650		86,217	2,968	.03442	.03817 ± .00093
500	500		86,217	3,631	.04211	.04596 ± .00107
200	250	Out	33,565	14,484	.4345	
200	350	No	33,565	13,556	.4039	
200	650	Atten.	33,404	13,144	.3935	
200	500		33,404	13,681	.4096	

TABLE V (continued)

R^2 = 70.09 cm^2. θ = 59° d_2 = 26.3 cm. d_4 = 29.2 cm.

Time in Sec.	E Div.	Scat-terer	Monitor Counts -Background	Detector Counts -Background	$\frac{\text{Detector-Background}}{\text{Monitor-Background}}$	δ_I
600	250	In	108,161	14,198	.13127	
600	350		108,161	12,428	.11490	
600	650		110,437	8,076	.07313	
600	500		110,437	10,108	.09800	
600	250	Out	112,345	6,709	.05972	.07155 ± .00090
600	350		112,345	5,571	.04959	.06531 ± .00084
600	650		113,986	4,000	.03509	.03804 ± .00067
600	500		113,986	4,707	.04129	.05671 ± .00078

TABLE V (continued)

R^2 = 56.34 cm^2 $\theta = 66^\circ$ d_2 = 25.0 cm. d_4 = 27.9 cm.

Time in Sec.	E Div.	Scat-terer	Monitor Counts -Background	Detector Counts -Background	$\frac{\text{Detector-Background}}{\text{Monitor-Background}}$	δI
300	250	In	50,778	7,729	.15221	
300	350		50,778	6,303	.12413	
300	650		52,093	4,083	.07838	
300	500		52,093	5,218	.10017	
400	250	Out	72,798	4,904	.06736	.08485 ± .00152
400	350		72,798	3,911	.05372	.07041 ± .00119
400	650		71,507	2,808	.03927	.03911 ± .00097
400	500		71,507	3,220	.04503	.05514 ± .00116
200	250	Out	39,615	18,917	.4775	
200	350	No	39,615	18,031	.4552	
200	650	Atten.	39,354	17,412	.4424	
200	500		39,354	17,924	.4554	

TABLE V (continued)

R^2 = 47.34 cm^2 $\theta = 73^\circ$ d_2 = 23.9 cm. d_4 = 26.8 cm.

Time in Sec.	E Div.	Scat-terer	Monitor Counts -Background	Detector Counts -Background	$\frac{\text{Detector-Background}}{\text{Monitor-Background}}$	δI
300	250	In	55,863	9,428	.16877	
300	350		55,863	7,585	.13578	
300	650		54,236	4,469	.08240	
300	500		54,236	5,598	.10322	
400	250	Out	73,801	5,094	.06902	.09975 ± .00136
400	350		73,801	4,166	.05645	.07933 ± .00119
500	650		93,324	3,802	.04074	.04166 ± .00094
500	500		93,324	4,549	.04874	.05448 ± .00105
300	250	Out	53,817	27,417	.5094	
300	350	No	53,817	26,392	.4904	
300	650	Atten.	52,372	25,191	.4810	
300	500		52,372	25,973	.4959	

TABLE V (continued)

R^2 = 37.03 cm^2 $\theta = 90^\circ$ d_2 = 21.9 cm. d_4 = 24.8 cm.

Time in Sec.	E Div.	Scat-terer	Monitor Counts -Background	Detector Counts -Background	$\frac{\text{Detector-Background}}{\text{Monitor-Background}}$	δ_I
600	250	In	99,614	20,394	.20473	
600	350		99,614	16,423	.16486	
600	650		114,682	11,082	.09663	
600	500		114,682	14,288	.12459	
600	250	Out	108,667	8,607	.07921	.12552 ± .00096
600	350		108,667	7,141	.06571	.09915 ± .00053
600	650		105,767	5,088	.04811	.03852 ± .00064
600	500		105,767	6,156	.05820	.06639 ± .00070
200	250	Out	35,689	20,677	.5794	
200	350	No	35,689	20,261	.5677	
200	650	Atten.	35,253	20,014	.5677	
200	500		35,253	20,747	.5885	

TABLE VI

With Attenuator

$K_1 = 31.89 \times 10^{-24}$ cm.^{2}/steradian

θ	$\left(\frac{d\sigma(\theta)}{d\omega}\right)_{650}$	$\left(\frac{d\sigma(\theta)}{d\omega}\right)_{500}$	$\left(\frac{d\sigma(\theta)}{d\omega}\right)_{350}$	$\left(\frac{d\sigma(\theta)}{d\omega}\right)_{250}$
28°	.6211	.5531	.6839	.6531
38°	.4662	.5546	.6320	.6676
39°	.4673	.4857	.5879	.6210
49°	.3135	.3619	.4691	.4976
57°	.2675	.3094	.3817	.4832
59°	.2352	.3396	.3939	.4060
66°	.2040	.2795	.3570	.4029
73°	.1821	.2309	.3400	.4116
90°	.1308	.2175	.3367	.4176

TABLE VII

With Attenuator $K_1 = 31.89 \times 10^{-24}$ cm./steradian

θ	$\left(\frac{d\sigma(\theta)}{d\omega}\right)_{250} - \left(\frac{d\sigma(\theta)}{d\omega}\right)_{350}$	$\left(\frac{d\sigma(\theta)}{d\omega}\right)_{350} - \left(\frac{d\sigma(\theta)}{d\omega}\right)_{500}$	$\left(\frac{d\sigma(\theta)}{d\omega}\right)_{500} - \left(\frac{d\sigma(\theta)}{d\omega}\right)_{650}$
28°	-.0308±.0385	.1308±.0411	-.0680±.0850
38°	.0347±.0082	.0783±.0171	.0884±.0129
39°	.0331±.0113	.1022±.0157	.0184±.0028
49°	.0285±.0068	.1072±.0130	.0484±.0089
57°	.1015±.0143	.0723±.0159	.0419±.0076
59°	.0121±.0024	.0543±.0073	.1044±.0098
66°	.0459±.0062	.0775±.0149	.0755±.0199
73°	.0716±.0064	.1091±.0070	.0488±.0054
90°	.0809±.0034	.1192±.0032	.0867±.0030

TABLE VII (continued)

θ	$\left(\frac{d\sigma(\theta)}{d\omega}\right)_{250} - \left(\frac{d\sigma(\theta)}{d\omega}\right)_{650}$	$\frac{d\sigma_{el}(\theta)}{d\omega}$	$k^2 \frac{d\sigma_{el}(\theta)}{d\omega}$
28°	.0320 ± .0110	.5352 ± .017	6.99 ± .23
38°	.2014 ± .0133	.3803 ± .008	4.96 ± .11
39°	.1537 ± .0174	.3814 ± .009	4.98 ± .12
49°	.1841 ± .0107	.2276 ± .006	2.97 ± .08
57°	.2157 ± .0089	.1616 ± .005	2.11 ± .07
59°	.1708 ± .0060	.1493 ± .003	1.95 ± .04
66°	.1989 ± .0080	.1181 ± .004	1.54 ± .05
73°	.2295 ± .0067	.0962 ± .003	1.26 ± .04
90°	.2868 ± .0037	.0449 ± .001	.59 ± .02

TABLE VIII

Monitor Background = 2240/400 sec. Detector Background (250) = 275/400 sec.

ΔE = 556 = 50 Divisions of E Detector Background (650) = 112/400 sec.

No Attenuator d_1 = 23.7 cm.

d_3 = 22.0 cm.

R^2 = 518.81 cm^2 $\theta = 30^\circ$ d_2 = 41.3 cm. d_4 = 44.2 cm.

Time in Sec.	E Div.	Scat-terer	Monitor Counts -Background	Detector Counts -Background	Detector-Background / Monitor-Background	δI
1200	650	In	301,159	59,831	.19867	
1200	650	Out	298,509	54,881	.18385	.01482 ± .00078
1200	250	In	296,548	67,778	.22856	
1200	250	Out	297,735	61,921	.20797	.02059 ± .00082
R^2 = 134.80 cm^2			$\theta = 45^\circ$		d_2 = 29.3 cm.	d_4 = 32.2 cm.
900	650	In	196,122	74,101	.37783	
900	650	Out	198,775	68,536	.34479	.03304 ± .00130
900	250	In	207,030	88,930	.42955	
900	250	Out	204,398	78,545	.38427	.04528 ± .00135

TABLE VIII (continued)

R^2 = 69.62 cm^2 $\theta = 60^\circ$ d_2 = 25.0 cm. d_4 = 27.9 cm.

Time in Sec.	E Div.	Scatterer	Monitor Counts -Background	Detector Counts -Background	$\frac{\text{Detector-Background}}{\text{Monitor-Background}}$	δI
900	650	In	215,454	104,877	.48677	
900	650	Out	211,407	94,358	.44633	.04044 ± .00141
900	250	In	210,855	119,258	.56559	
900	250	Out	208,196	101,704	.48850	.07709 ± .00152

R^2 = 46.37 cm^2 $\theta = 75^\circ$ d_2 = 22.5 cm. d_4 = 25.4 cm.

900	650	In	219,966	124,498	.56599	
900	650	Out	219,826	114,904	.52270	.04329 ± .00149
900	250	In	224,004	147,130	.65682	
900	250	Out	220,121	121,869	.55365	.10317 ± .00157

TABLE VIII (continued)

Time in Sec.	E Div.	Scatterer	Monitor Counts -Background	Detector Counts -Background	Detector-Background / Monitor-Background	δI
R^2 = 42.65 cm^2.			$\theta = 80^\circ$	d_2 = 21.9 cm.		d_4 = 24.8 cm.
900	650	In	217,651	132,237	.60756	
900	650	Out	210,542	120,029	.57010	.03746 ± .00159
900	250	In	211,748	151,232	.71421	
900	250	Out	205,219	122,079	.59487	.11934 ± .00169
R^2 = 34.80 cm^2.			$\theta = 103^\circ$	d_2 = 19.3 cm.		d_4 = 22.2 cm.
900	650	In	248,364	185,440	.74665	
900	650	Out	244,449	169,774	.69452	.05213 ± .00164
900	250	In	241,920	211,176	.87292	
900	250	Out	237,463	171,799	.72348	.14944 ± .00176

TABLE IX

Without Attenuator $K_2 = 26.71 \times 10^{-24} cm.^2/steradian$

θ	$\left(\frac{d\sigma(\theta)}{d\omega}\right)_{650}$	$\left(\frac{d\sigma(\theta)}{d\omega}\right)_{250}$	$\left(\frac{d\sigma(\theta)}{d\omega}\right)_{250} - \left(\frac{d\sigma(\theta)}{d\omega}\right)_{650}$	$\frac{d\sigma_{el}(\theta)}{d\omega}$	$k^2 \frac{d\sigma_{el}(0)}{d\omega}$
30°	.5718	.7025	.1305 ± .0256	.495	6.46 ± .35
45°	.3328	.4092	.0764 ± .0117	.256	3.34 ± .19
60°	.2164	.3770	.1606 ± .0092	.140	1.82 ± .11
75°	.1590	.3577	.1987 ± .0074	.082	1.08 ± .07
80°	.1321	.4031	.2710 ± .0070	.055	.71 ± .04
103°	.1416	.3897	.2481 ± .0062	.065	.85 ± .06

BIBLIOGRAPHY

1. Allred, J. C. and Armstrong, A. H., "Laboratory Handbook of Nuclear Microscopy (Tentative)", Los Alamos Scientific Laboratory of the University of California, Nov., 1951.
2. Baldinger, Huber and Staub, Helvetia Physica Acta 11, 245 (1938).
3. Barschall and Ladenburg, Phy. Rev. 61, 129 (1942).
4. Barschall, Manley and Weisskopf, Phy. Rev. 72, 875 (1947).
5. Barschall, H. H. and Taschek, R. F., Phy. Rev. 75, 1819 (1949).
6. Bonner, T. W., Phy. Rev. 52, 685 (1937).
7. Brundage, R. S., "Total Cross Section of Aluminum for D(d,n) Neutrons", unpublished M. A. Thesis, University of Texas, June, 1952.
8. Coon, J. H. and Barschall, H. H., Phy. Rev. 70, 592 (1946).
9. Day, R. B., Phy. Rev. 89, 908 (1953).
10. Dvorak, H. R., "Total Cross Sections of Bromine, Chlorine, Sodium and Titanium", Ph. D. Dissertation, University of Texas, May, 1953 (to be published).
11. Elliot, L. G. and Deutsch, M., Phy. Rev. 63, 321 (1943).

12. Falk, C. E. and Poss, H. L., Am. Jour. Phy. 20, 429 (1952).

13. Feld, Feshbach, Goldberger, Goldstein, Weisskopf, "Final Report of the Fast Neutron Data Project", NYO-636, U. S. Atomic Energy Commission (1951).

14. Hofstadter, R., Nucleonics 6, No. 5, 70 (1950).

15. Jordan W. H. and Bell, P. R., Nucleonics 5, No. 4, 30 (1949).

16. Kallmann, H. and Furst, M., Phy. Rev. 79, 857 (1950).

17. Kruger, Shoupp and Slattman, Phy. Rev. 52, 678 (1937).

18. Leonard, Jr., B. P., "The Differential Angular Scattering of Neutrons from Aluminum and Copper", Ph. D. Dissertation, University of Texas, May, 1953 (to be published).

19. Miller, D. W., Adair, R. K., Bockelman, C. K., Dardes, S. F., Phy. Rev. 88, 83 (1952).

20. Schaeffer, N. M., "Scattering of D(d,n) Neutrons from Plane Slabs", Ph. D. Dissertation, University of Texas, May, 1953 (unpublished).

The vita has been removed from the digitized version of this document.